FLOOD ROUTING THROUGH STORM DRAINS

Part II

PHYSICAL FACILITIES AND EXPERIMENTS

by

V. YEVJEVICH and A. H. BARNES

November 1970

HYDROLOGY PAPERS
COLORADO STATE UNIVERSITY
Fort Collins, Colorado

44

Several departments at Colorado State University have substantial research and graduate programs oriented to hydrology. These Hydrology Papers are intended to communicate in a fast way the current results of this research to the specialists interested in these activities. The papers will supply most of the background research data and results. Shorter versions will usually be published in the appropriate scientific and professional journals, or presented at national or international scientific and professional meetings and published in the proceedings of these meetings.

The investigations leading to this paper on unsteady free-surface flow in a long storm drain were supported by the U.S. Bureau of Public Roads, Federal Highway Administration during 1960-1970 and by the Public Health Service during 1962-1964. The research was conducted in the Hydrology and Water Resources Program of Civil Engineering Department at Colorado State University, Fort Collins, Colorado, U.S.A.

The opinions, findings, and conclusions expressed in this publication are those of the authors and not necessarily those of the Federal Highway Administration or the Public Health Service.

Dr. Arthur T. Corey, Professor, Agricultural Engineering Department

Dr. Robert E. Dils, Professor, College of Forestry and Natural Resources

Dr. Vujica Yevjevich, Professor, Civil Engineering Department

FLOOD ROUTING THROUGH STORM DRAINS

Part II

PHYSICAL FACILITIES AND EXPERIMENTS

by

V. Yevjevich and A. H. Barnes

HYDROLOGY PAPERS
COLORADO STATE UNIVERSITY
FORT COLLINS, COLORADO 80521

November 1970 No. 44

ACKNOWLEDGMENTS

The writers of this paper gratefully acknowledge the support and cooperation of the U. S. Bureau of Public Roads, Federal Highway Administration, in the research on flood movements through long storm drains conducted from 1960 to 1970. The writers also acknowledge the U. S. Public Health Service, National Institute of Health, for their additional support during 1962-1964.

The initiative, cooperation and support given by Mr. Carl F. Izzard to this project on flood movement through storm drains is particularly acknowledged. Mr. Izzard, presently Director, Office of Development, Federal Highway Administration, U. S. Department of Transportation, and Chief, Hydraulic Research Division, U. S. Bureau of Public Roads at the start of the project. Further acknowledgment is extended to Mr. Charles F. Scheffey, Director, Office of Research, Federal Highway Administration, for his cooperation and encouragement. Dr. Dah-Cheng Woo, Senior Hydraulic Engineer, Federal Highway Administration, has cooperated extensively with this project. His reviews and suggestions pertaining to all reports, theses and other documents produced on the project have been particularly helpful.

Mr. George Smith, Associate Professor of Civil Engineering at Colorado State University, has worked closely with the writers in the design, construction, testing, and operation of the physical research facilities during most of this project. His contribution, particularly for the material included in this paper, is acknowledged. Several graduate students, either through their thesis research or through direct work, contributed to the project. The theses and reports are listed in the bibliography of this paper under "Internal References". Acknowledgment is also given to Mr. Lawrence Wetter, Project Engineer, Soil Conservation Service, Winfield, Kansas, and Mr. Don Signor, Hydrologist, Geological Survey, Lubbuck, Texas, for their contributions in the design and testing of the orifice meters, junction boxes, and the model study of inlet and outlet conditions during their M.S. graduate studies at Colorado State University. Particular acknowledgment is extended to the mechanics and other shop specialists of the Engineering Research Center, who have made it possible to construct, maintain and operate these unique facilities and the instrumentation described in this paper. Dr. Shih-Tun Su, Post Doctoral Fellow, Civil Engineering Department, Colorado State University, using existing data, assisted the writers in finishing this paper.

TABLE OF CONTENTS

LIST OF FIGURES AND TABLES

ABSTRACT

This second part of a four-part series of hydrology papers on flood routing through storm drains relates exclusively to experimental research facilities and experiments. The following subjects are presented: (a) design and construction of the experimental storm drain system as a special conduit research outdoor facility; (b) instrumentation and its calibration; (c) description of the data recording system; (d) various experimental test conditions and their typical results, and (e) discussion of experimental errors.

A large conduit, 3 feet in diameter and 822 feet long, was selected, designed, and constructed in the Outdoor laboratory at Colorado State University, Engineering Research Center, to accurately measure geometric and hydraulic characteristics, as well as the propagation of flood hydrographs. Instrumentation was selected to suit the field conditions. The calibration of the instruments was carried out to the point where there were relatively small errors. The data recording system was designed and constructed so that the output could be put either on cards or paper tapes and provide a direct input for computations on a digital computer. Only typical results of experiments carried out are described in this paper; experimental errors are reviewed in a summarized form.

FLOOD ROUTING THROUGH STORM DRAINS

Part II

PHYSICAL FACILITIES AND EXPERIMENTS

by

V. Yevjevich* and A. H. Barnes**

Chapter 1

INTRODUCTION

1.1 Objectives in the Use of Physical Research Facilities

One of the main objectives of investigating flood routing through storm drains was to compare analytical and physical waves, or to compare waves computed by integrating the two quasi-linear hyperbolic partial differential equations of gradually varied free surface unsteady flow and the corresponding free-surface waves measured in a conduit. Therefore, constructing appropriate facilities to simulate and measure the physical waves became necessary. These new facilities have the objectives:

(1) To physically simulate and measure free-surface waves at various points along the research conduit for the comparisons discussed.

(2) To measure various geometric and hydraulic characteristics of the conduit and the waves in order to analyze these characteristics, so that the analytical waves-as the inflow flood hydrographs routed along the conduit by the integration of the two De Saint-Venant partial differential equations-may come as close to the corresponding physical waves as practically feasible.

(3) To physically simulate a storm drain with lateral inflows joining the main conduit at junction boxes.

(4) To study boundary and initial conditions in the experimental conduit, so that their uses in the integration of differential equations represent the real conditions of physical waves as much as practically feasible.

1.2 General Conceptions for the Physical Research Facilities

Most hydraulic research and the development of hydraulic formulas in the past have been done on relatively small laboratory experimental facilities. Economy was the primary reason research facilities were relatively smaller than the prototypes they represented. Most hydraulic formulas and related computational methods have been developed by using the computational devices available. For economy of computations in the pre-computer age required simplified formulas and tractable computational methods to treat the often complex hydraulic problems of nature.

The advent of fast digital, analog, and hybrid computers, however, has reduced substantially the unit cost of numerical solutions of complex problems, formulas, and methods. The availability of electronic computers has made many previous hydraulic mathematical models and corresponding computational methods obsolete. With time, these models and formulas are likely to be completely revised and upgraded. Versatile improvements of many hydraulic computational methods are progressing and are expected to come about in the near future.

One of the expected contributions of this research project on flood routing through storm drains is an improved base for replacing less reliable steady-state conditions by more reliable unsteady free-surface flow conditions in the design of storm drains. Therefore, the advanced methods, simulating natural conditions as closely as feasible, may be introduced in the form of unsteady-flow approach to the design of storm drains. Improving computational flood routing methods through storm drains is meaningful only if the accuracy of input flood hydrographs and the accuracy of geometric and hydraulic parameters in differential equations becomes much greater than their accuracy in the steady-flow peak-discharge approach for design of storm drains.

The two partial differential equations of gradually varied free-surface unsteady flow are developed from several basic assumptions. Even with these assumptions there will always be a difference between the analytically computed wave at a given position of a free-surface flowing storm drain for a given inflow flood hydrograph, and the physical wave observed at the same position and for the same inflow hydrograph. To study the geometric and hydraulic characteristics of conduits and waves in order to integrate flood waves moving through storm drains, and to compare the analytical and the physical waves, small scale facilities did not appear feasible. Relative errors that appear when various hydraulic and geometric parameters are measured in small scale facilities are usually large. To decrease these errors, and to better study various aspects of flood movement through storm drains, larger scale physical research facilities were conceived, designed, and built.

Because of the potential of various numerical computations being reliably performed by digital, analog, and hybrid computers, the science of hydraulic is now in the position of re-evaluating previously developed formulas and computational methods. When the objective becomes an assessment of the accuracy of presently available formulas and computational methods in hydraulics, not only or predominantly the development of the new hydraulic regularities and laws, the most feasible way of checking the existing mathematical hydraulic models and the computational methods is

* Professor of Civil Engineering and Professor-in-Charge of Hydrology and Water Resources Program, Civil Engineering Department, Colorado State University, Fort Collins, Colorado.
**Associate Professor of Civil Engineering, Civil Engineering Department, Colorado State University.

through facilities of sufficiently large scale. For mainly that purpose, an outdoor laboratory was built at the Engineering Research Center of Colorado State University. Several large scale facilities already have been built in this outdoor laboratory. One of them is the conduit research facility having a pipe 822 feet long with an inside nominal diameter of 3 feet. This conduit can be moved on inclined rails to obtain slopes from 0 to 4 percent. This facility, with auxiliary apparatus, represents the conduit research center and will be used primarily for the study of the free-surface water flow through storm drains, and also for future objectives. A significant study on the diffusion of tracers in a full flowing pipe has also been performed in these facilities.

It is expected that the conduit research facilities will be used for other problems, e.g. water transport of materials in pipes, pre-treatment of sewage water in drainage systems, problems in separating sewage water from storm-drain water of the same drainage system, studies of pipe roughness, studies of various diffusion problems, investigations of losses at hydraulic singularities along conduits, etc. These facilities are available to both researchers in the United States and to guests from foreign universities. These facilities are described in Chapter 2.

A detailed description of facilities, instruments, the calibration of instruments, methods, and typical experimental results was considered necessary in a special hydrology paper for two reasons.

(1) That an assessment of the value of results and conclusions in this investigation of flood routing through storm drains can be made by those who read and study the four parts of this research project, published as the Colorado State University Hydrology Papers, Nos. 43-46.

(2) That the scientists who would like to perform various research projects at the CSU conduit research center may assess advantages, potential, and limitations in using these facilities for particular research problems.

1.3 Organization of Material Included in this Paper

The general description of various alternatives in planning the research facilities, and the details of the constructed storm drain system are described in Chapter 2. The instruments used in the experiments are described in Chapter 3, with a major emphasis on calibration of individual devices. Chapter 4 describes the data recording system which allows data taken in the field to be transmitted to an indoor analog-to-digital converter located approximately 1/4 mile from the pipeline. Chapter 4 describes how the output from the analog-to-digital converter, in the form of punched cards or tapes, may be fed directly into the computer. Various experimental test conditions and their typical results are described in Chapter 5 such as flow resistance, cross-sectional velocity distribution, box losses, initial and boundary conditions, and observations of propagated flood waves. Experimental errors caused by different sources are discussed in Chapter 6. Chapter 7 presents the general evaluation of experimental facilities; it is followed by the references (external and internal).

Chapter 2

EXPERIMENTAL STORM DRAIN SYSTEM

2.1 Description of Circular Conduit

A pipeline 822 feet long with a 3-foot diameter was used as the experimental conduit in this study as shown in Figs. 2.1 and 2.2.

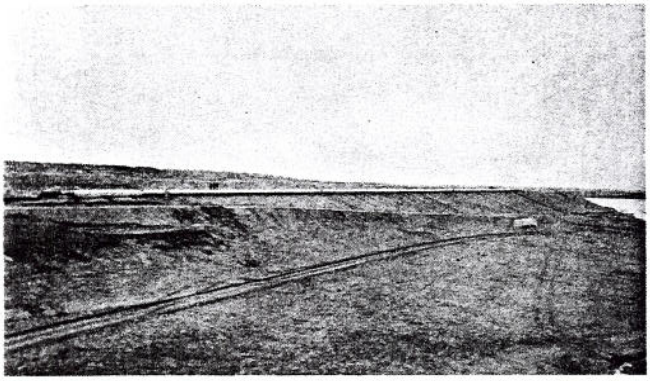

Fig. 2.1. The circular conduit on the hillside of the Outdoor Laboratory at Colorado State University Engineering Research Center.

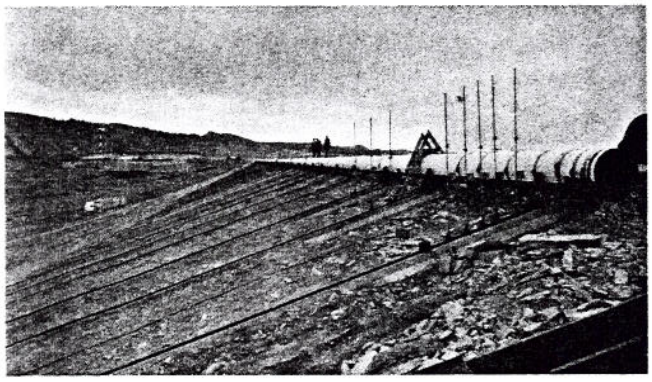

Fig. 2.2. View from the outlet of circular conduit and the inclined rails.

The entire 822 feet of pipe, which consisted of 20-foot sections, was supported on inclined rails which permitted the pipe to be moved along the inclined plane to any slope between 0 and approximately 4 percent. Figures 2.3 and 2.4 display general layout and detailed designs of the circular storm conduit.

The pipe material is 1/2 inch thick rolled steel plate with a longitudinal weld located at the crown. The approximate 20-foot lengths of the pipe were welded except at three positions where the connections were bolted. Extreme care was taken to insure that all inside welds and joints were ground smooth and that the depressions were filled with a plastic material to insure a uniformly smooth surface. The inside surface was sand blasted and painted with two coats of a rust preventative paint.

2.2 Inlet Structure

Selection of inlet structure. Flow was introduced into the circular storm conduit by means of an inlet structure. Two inlet structures were initially designed, as shown by Figs. 2.5 and 2.6. The design details of these two schemes, their cost estimates, advantages, and disadvantages are presented in Table 2.1. The advantage of lower cost and added convenience in operation led to the selection of the second scheme as the inlet structure to be constructed.

Model study of selected inlet structure. A model study was made of the selected inlet structure (scheme No. 2). The length ratio of model to prototype was 1 to 6. The objectives of this study were:

1. To investigate the problems of controlling the water profile in the main pipe line for both subcritical and supercritical flow by one or more of the following methods:
   a. Varying the grid size, number, and position of baffles in the inlet section of the intake structure.
   b. Varying the slope of the intake structure only.
   c. Use of a tailgate at the point of discharge from the main pipe for subcritical flow.
2. To investigate the hydraulic performance of the inlet box for subcritical and supercritical flows.

A schematic diagram of the model study with design details is shown in Fig. 2.7. The types of baffles tested are also shown in the figure.

Conclusions of the model tests are as follows:

1. For subcritical flow the use of baffles and a tailgate is an effective method for developing uniform flow in the main conduit. It was necessary, however, to double the length of the intake structure between the flexible pipe and the main pipe line. This permitted full development of a uniform flow before entry into the main pipe.
2. By keeping the invert of the intake structure above the crown of the supply pipe, full pipe flow is always maintained at the orifice meter.
3. Varying only the slope of the intake structure is as effective as baffles in developing uniform flow in the main pipe for subcritical flow.

Description of inlet structure as constructed. On the basis of the experimental results of the model study, the inlet structure was constructed following the design of scheme No. 2. For subcritical flow conditions it was necessary that the desired flow characteristics be developed upstream of the entrance to the storm conduit. This required that the 22-foot approach section have freedom of movement both vertically and horizontally so that it could be oriented in any given plane with the storm conduit. The flexible section of pipe was built to allow the desired freedom of orientation of the 22-foot approach section to be a straight continuation of the storm conduit in any experiments.

The movement of the storm conduit relative to the fixed portion of the intake structure created undesirable secondary currents in the approach section to the storm conduit. To re-align these transverse

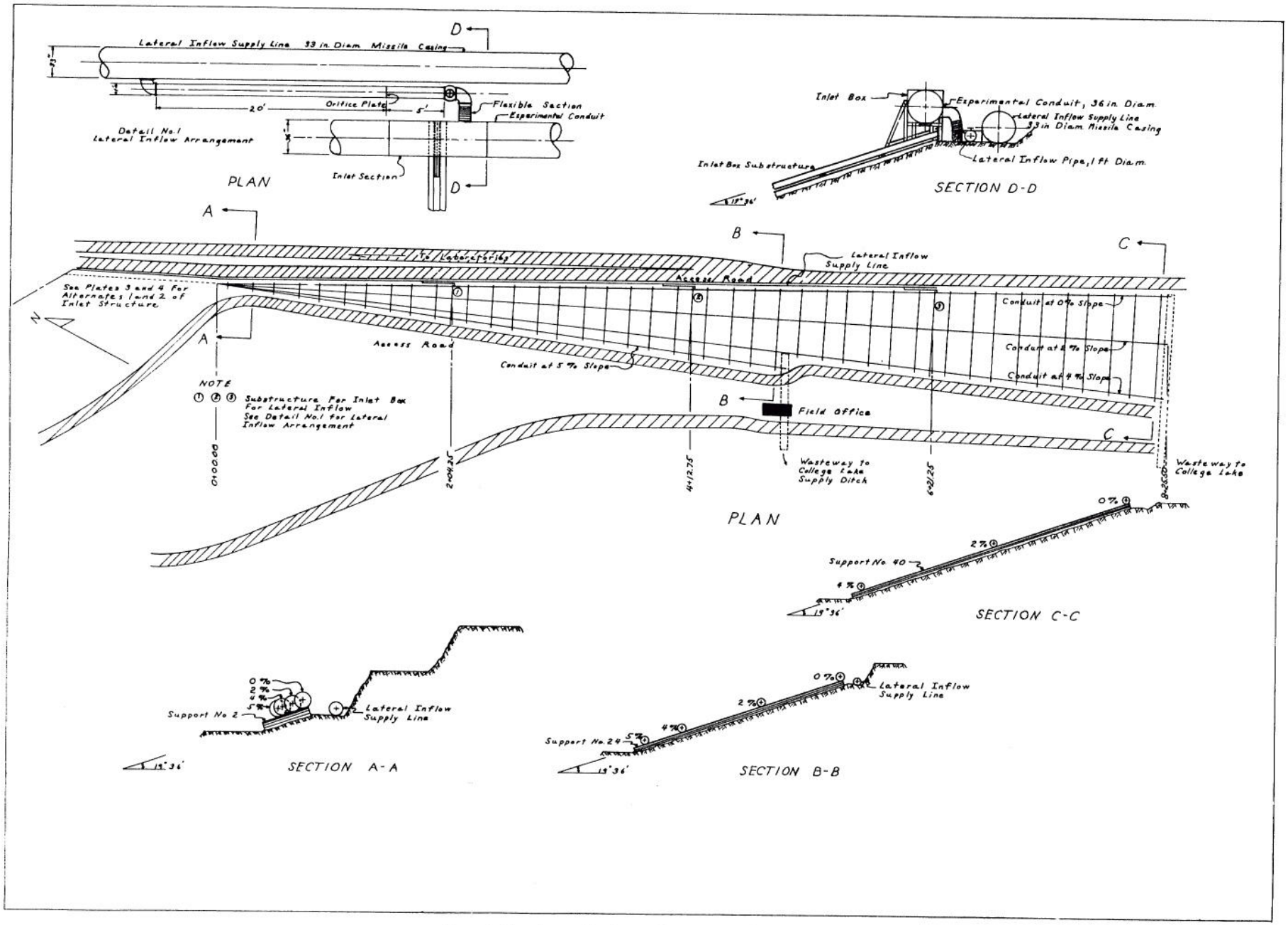

Fig. 2.3. General plan of storm conduit experimental facilities.

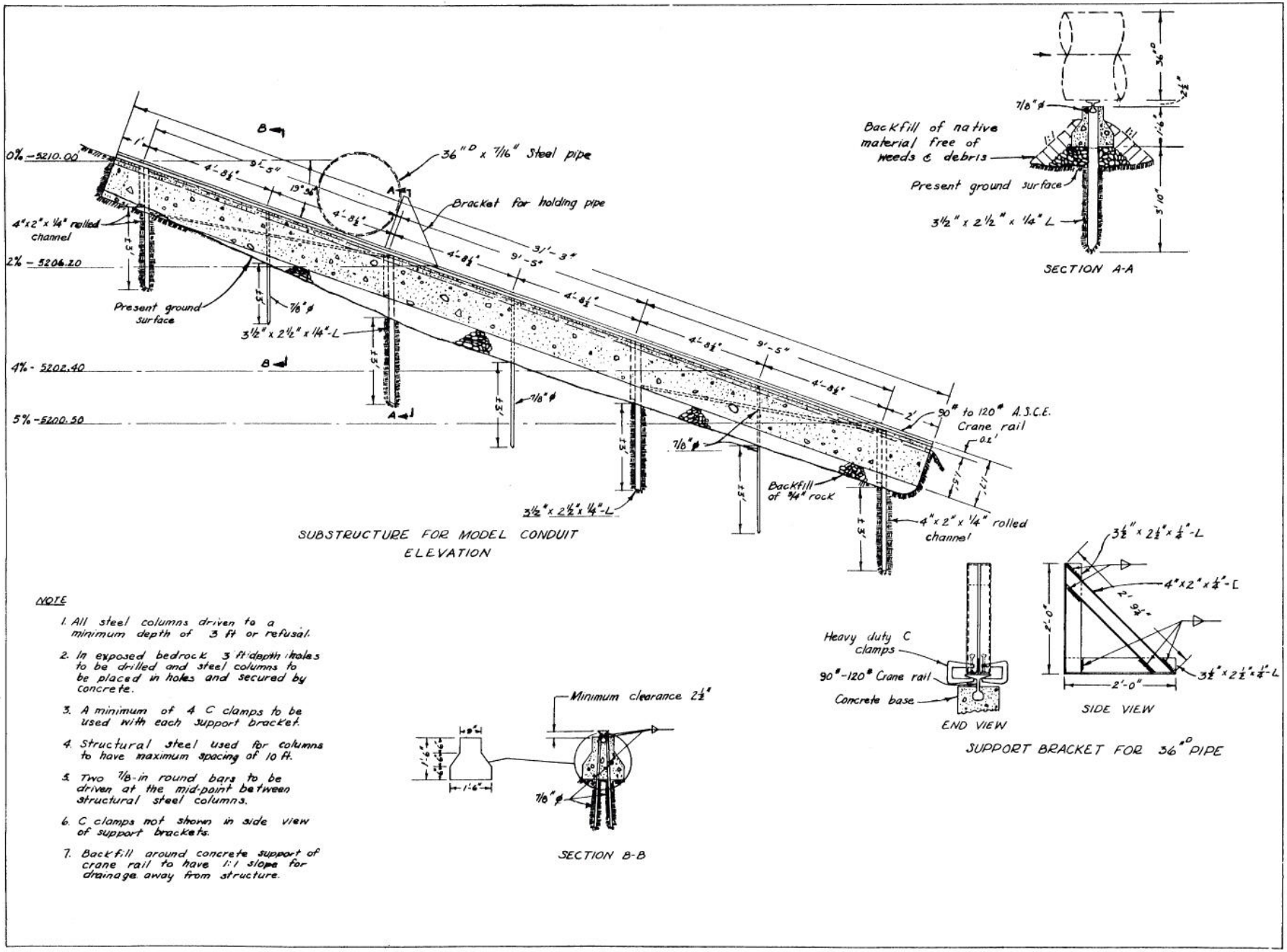

Fig. 2.4. Substructure for storm conduit experimental facilities.

TABLE 2.1. Design details, cost, advantages, and disadvantages of the two schemes of inlet structure.

	SCHEME NO. 1	SCHEME NO. 2
Design details	(1) A 30-foot section of 26-inch diameter pipe. (2) A 5-foot transition section with guide vanes. (3) An 8-foot by 10-foot by 58-foot stilling basin with baffles at the entrance and a triangular weir at the exit. (4) A 10-foot by 10-foot catchment box. (See Fig. 2.5)	(1) An 80-foot section of 26-inch diameter pipe with orifice meter. (2) An 12.25-foot of steel pipe between the orifice meter and a length of flexible pipe. (3) A 10-foot of 26-inch diameter flexible pipe. (4) A 3-foot transition section between the flexible pipe and, (5) A 22-foot missile case with baffles. (See Fig. 2.6)
Estimate of cost	$3850.00	$2300.00
Advantages	(1) It provides an accurate measurement of discharge from very low to maximum discharge. (2) Flood waves - inflow hydrographs - can be easily generated in the stilling basin with the addition of a relatively expensive wave generator.	(1) It is relatively inexpensive. (2) It provides positive control of the flow phenomena without interference, that is, the water surface is not affected by the wind. (3) Because it is a single pipe system a valve can be easily installed in the system at any time if it be found desirable, which is a desirable feature for a limited water supply. (4) It permits the use of several sizes of orifice meters for measuring a wide range of flow discharges.
Disadvantages	(1) Wind will cause surface waves, which will have an adverse effect on the discharge measurements, particularly at low discharge. (2) Its cost is high. (3) Calibration of the weir may require double construction of the stilling basin. (4) It is cumbersome to operate.	(1) For supercritical flows it might not be easy for some discharges to develop desired uniform flow. (2) There is a danger of the flexible pipe collapsing during movement of the pipe system.

velocity components into the desired uniform flow it is necessary to place baffles in the approach section. The location and number of these baffles is determined by observing the flow developed for a given discharge.

To develop the desired supercritical flow conditions at the entrance to the storm conduit, it was necessary that the slope of the movable approach pipe be different than the slope of the storm conduit. To achieve this slope differential, a flexible coupling was installed at the junction of the two pipes, i.e., at the entrance to the storm conduit.

2.3 Laterals and Junction Boxes

Selection of junction box. The design of laterals for the lateral inflows into the storm conduit, and the junction boxes basically involves three factors: (1) The angle of intersection; (2) The vertical position of the lateral inlet in the cross-section of the main conduit, and (3) The shape of junction box. If the crown of the inlet pipe is at the same elevation as the crown of the main conduit, it is referred to as the "upper inlet". If the invert of the inlet pipe is at the same elevation as the invert of the main conduit, it is referred to as the "lower inlet".

Based on recommendations from the U. S. Bureau of Public Roads, a square box with a changeable upper and lower inlet, and an angle of intersection equal to 90 degrees was selected as the junction box. Design details are shown in Figs. 2.8 and 2.9.

A model study of the selected junction box with its two positions, i.e., the upper and lower inlets, is described in the next section.

Model study of selected junction box. A hydraulic model was made to determine the relation of the power loss at the junction to other hydraulic properties.

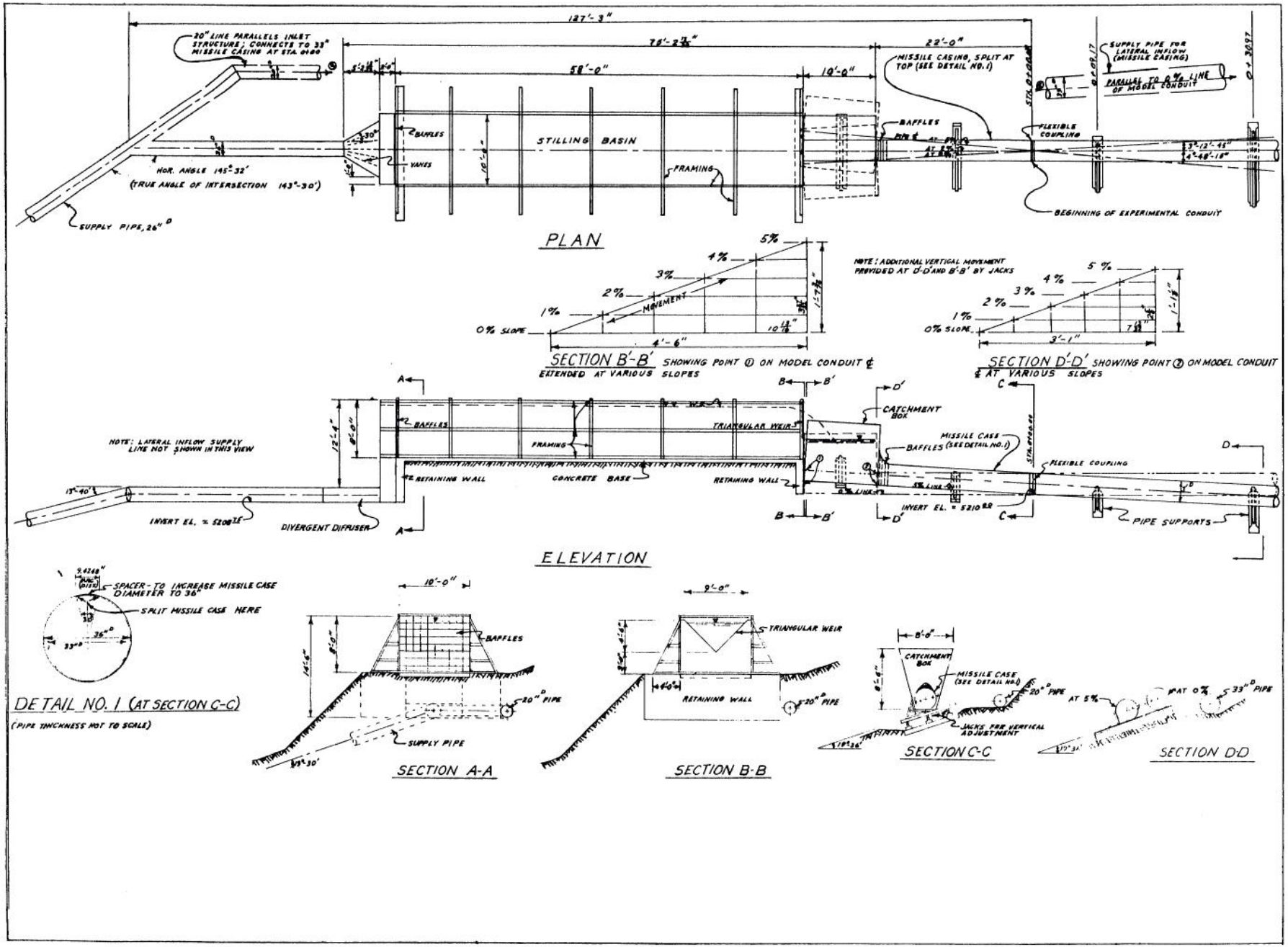

Fig. 2.5. Inlet structure, scheme No. 1.

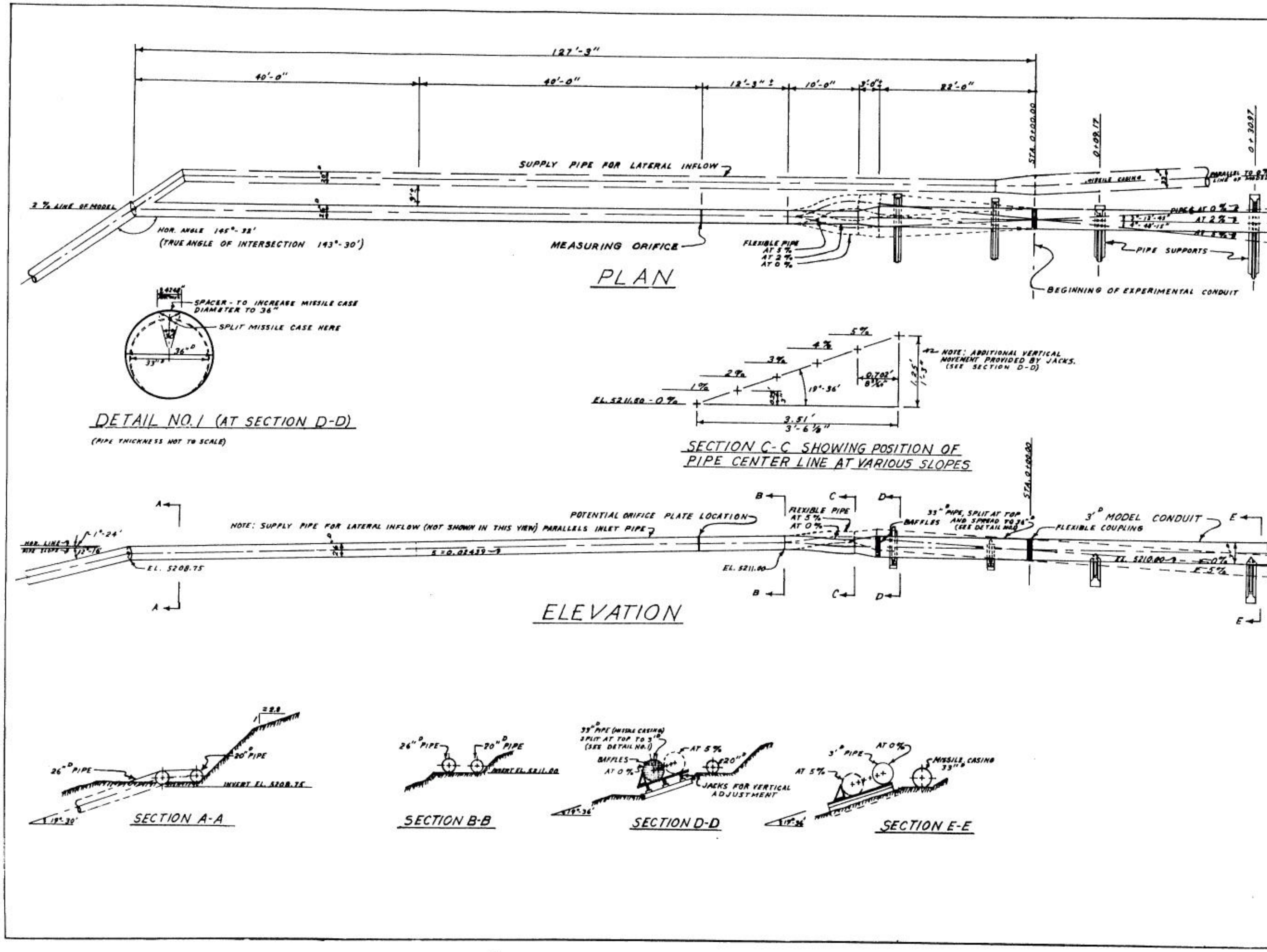

Fig. 2.6. Inlet structure, scheme No. 2.

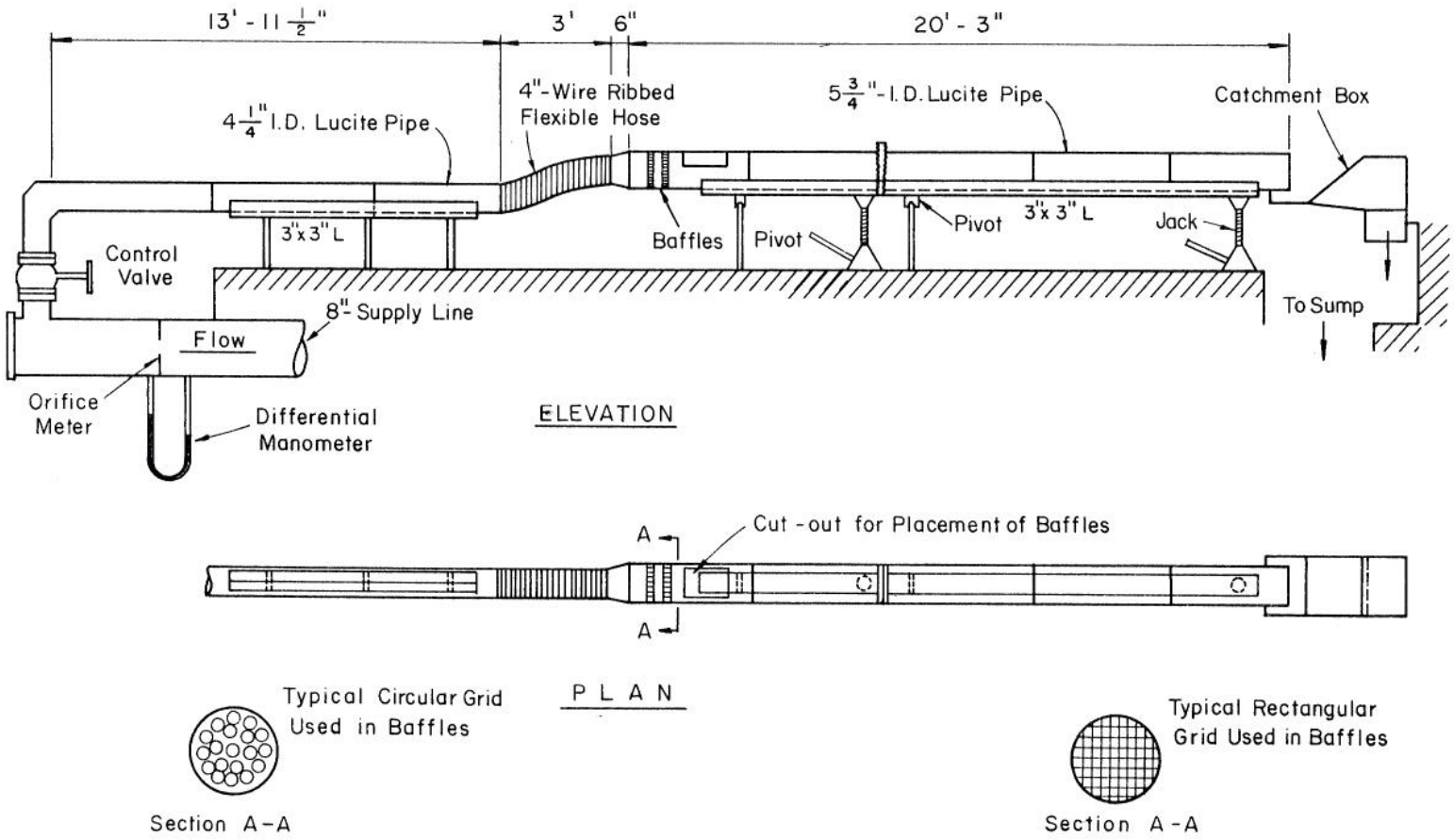

Fig. 2.7. Schematic diagram showing experimental set-up for model study of storm drain -- intake structure, main pipe line and outlet.

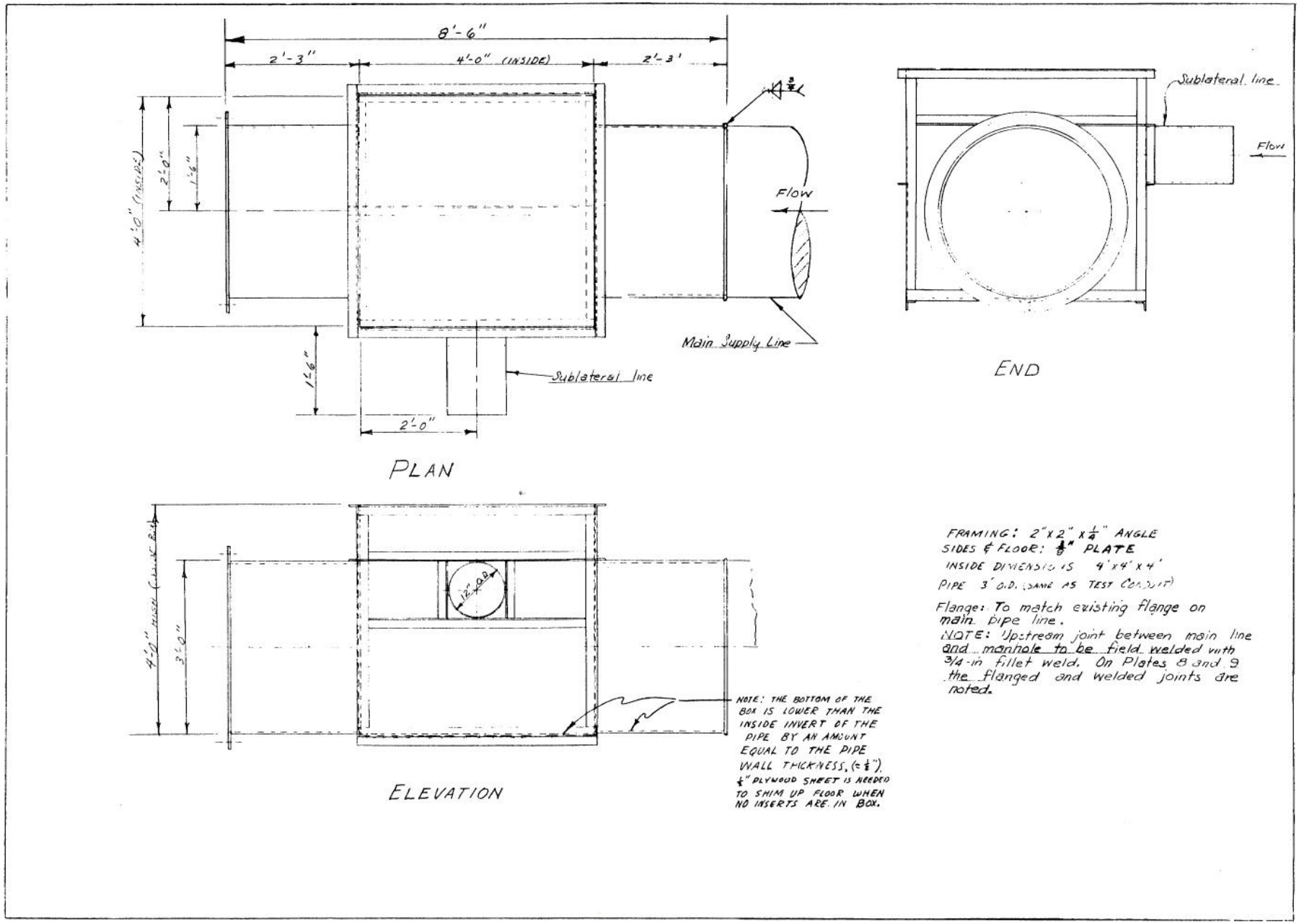

Fig. 2.8. Junction box at 90° with the upper inlet.

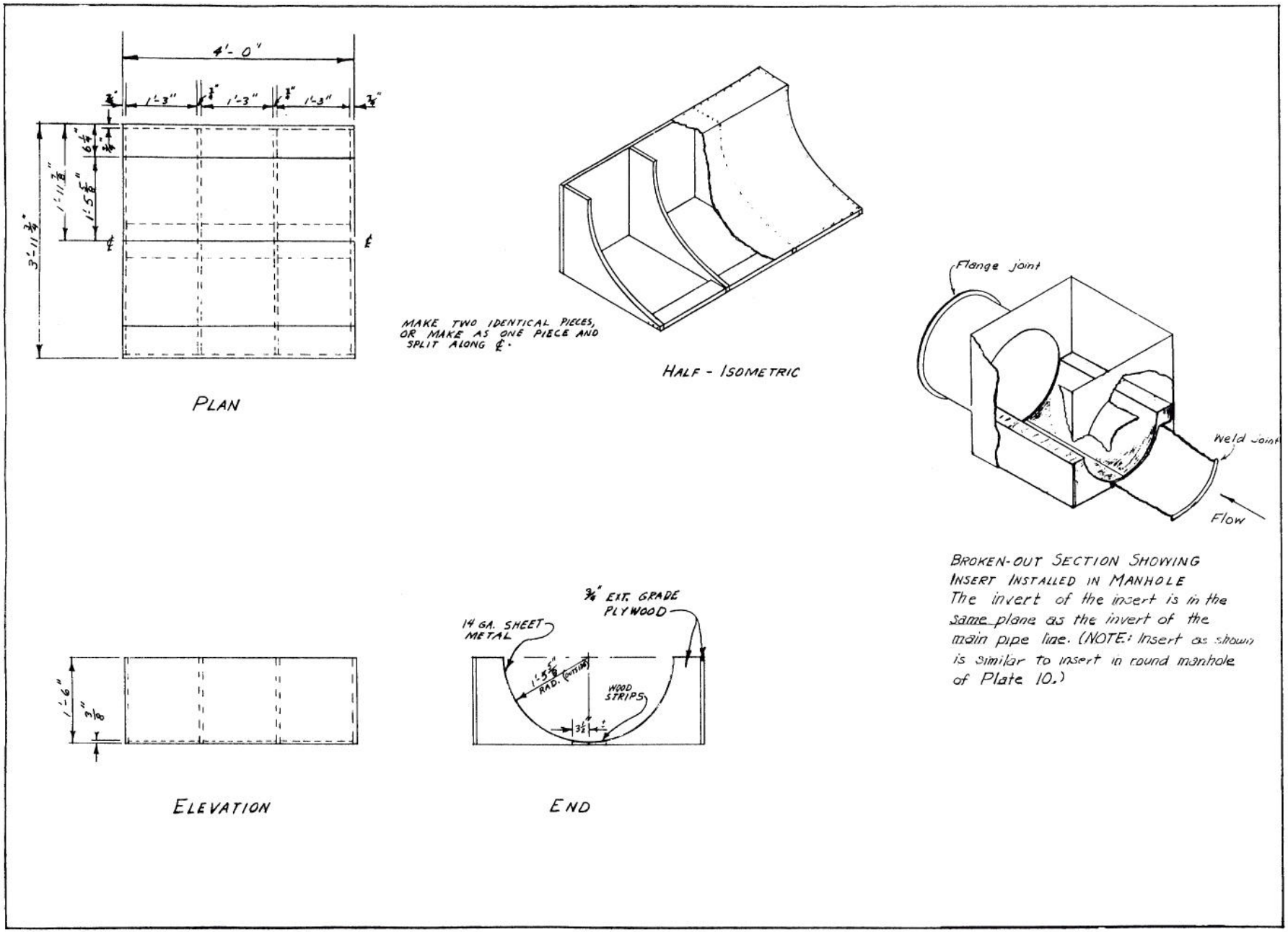

Fig. 2.9. Details of the junction box.

Froude modeling criteria were used with a model to prototype linear ratio of 1 to 5.618 (selected because of the available plastic pipe size).

The junction box used in the model study was square above the half-full level of the storm conduit. The two positions of the inlet were tested, the upper inlet and the lower inlet. The crown of the upper inlet was at the same elevation as the crown of the storm conduit at its point of entry into the junction box. The invert of the lower inlet was made coincident with the invert of the storm conduit at their junction point, which was the centerline of the junction box. The lower inlet had a horizontal slope of 0.05. This slope was a result of necessary structural details in the prototype. Details of the model junction box are shown in Figs. 2.10, 2.11 and 2.12.

When the upper inlet was used, the lower inlet was plugged. Depths of water were measured at 22 points along the model conduit. The rate of main flow and the rate of lateral flow were read from two calibrated manometers. The measured depths were used to calculate the cross-sectional areas. The mean velocities were then calculated by the continuity equation. Then the velocity heads were calculated. Knowing the velocity heads, depth of flow, and the elevation of the invert, energies could be calculated for each station. The power at a section in the conduit is found by multiplying the energy at the section by the weight rate of flow past the section. In other words, this power is the energy for all of the water transmitted across a section per unit time. The power equation can be written as:

$$P = Q\,\gamma(z + y + V^2/2g) \qquad (2.1)$$

or

$$P = Q\,\gamma\,E \quad , \qquad (2.2)$$

in which P is the power in foot-pounds per second, Q is the rate of flow in cfs, γ is the specific weight of water in pounds per cubic foot, E is the energy in foot-pounds per pound, V is the mean velocity, z is the elevation of the bottom, and y is the depth of water in the model conduit.

Conclusions drawn from this model study for subcritical flow are:

1. For a given ratio of lateral to main flow there is always more power lost when the upper inlet is utilized than when the lower inlet is used.
2. The ratio of power loss to the incoming power for the upper inlet is dependent only on the ratio of lateral to main flow.

The power loss relation for the upper lateral inlet (the inlet that had its crown at the same elevation as the crown of the storm conduit) was found to be:

$$P_R = \frac{-0.482}{Q_R + 0.55} + 0.77, \qquad (2.3)$$

in which P_R is the ratio of power loss in the junction to the power entering the junction, and Q_R is the ratio of lateral inflow to storm conduit inflow. This equation is valid for Q_R greater than 0.10. For Q_R less than 0.10 the P_R-value of zero can be assumed with a maximum expected error of 3 percent in P_R.

3. The ratio of power loss to the power entering the lower inlet depends on the ratio of lateral to main discharge and the depth ratio of the junction.

The power loss relation for the lower lateral inlet (the inlet that had its invert at the same elevation as the storm conduit's invert) was found to be:

$$P_R = \frac{-2.78 + 1.71\,D_R}{Q_R + 3.122 - 0.167 D_R} + 0.77 \quad , \qquad (2.4)$$

in which P_R and Q_R are the same magnitudes as for the upper inlet, and the new parameter, D_R, is equal to the ratio of the depth immediately upstream from the junction box to the diameter of the storm conduit. This equation is limited to D_R-values greater than 0.5.

4. For a given flow ratio, Q_R, the power loss for the lower inlet increases as the depth upstream from the junction increases.

5. The slope of the main conduit does not affect the power loss ratio for the subcritical flow conditions.

6. The effective friction factor downstream from the junction has a larger value than the friction factor upstream.

Description of junction box as constructed. The constructed junction box had both upper and lower lateral inlets and was square in shape. Flow from the 12 inch lateral pipe entered into the square junction box at a 90-degree angle as a free fall jet of water for the upper lateral inlet.

2.4. Outlet Restriction Gate

A restriction gate with five movable vertical wooden slats was installed at the end of the 3 ft diameter, 822 ft long conduit. The five 7-inch vertical wooden slats were held in position by 2.5-inch wide vertical aluminum H-sections. The clear opening was 5 inches between supports. The detailed dimensions of the gate is shown in Fig. 2.13. During the experiments, the flow discharge could thus be controlled by varying the vertical position or by removing one or more of the slats to give the backwater (M1) profile. For the condition of a free outfall, the gate could be completely removed as shown in Fig. 2.14. A discussion of the gate condition is given in Chapter 5, p. 30.

2.5. Water Supply and Removal

Water supply to the 3-foot diameter storm conduit was by gravity from the nearby Horsetooth Reservoir (Colorado Big Thompson Project) through a 26-inch underground pipeline as shown in Figs. 2.15 and 2.16. The conduit flow discharged into College Lake. This system permits wide variation in the discharge demand on the water supply.

The monthly maximum, average, and minimum water surface elevations of Horsetooth Reservoir from May 1951 to September 1962 were obtained from records kept at the Northern Colorado Water Conservancy District, Loveland, Colorado. These values were plotted on the graph presented in Fig. 2.17. The mean 11-year reservoir surface elevation for this period is 5382 feet above mean sea level. The differential elevation between the inlet of storm conduit and reservoir water surface provides the maximum available head. A rating curve was then prepared as indicated in Fig. 2.18. From the rating curve of Fig. 2.18, a discharge of 90 cfs was obtained for the mean 11-year reservoir surface elevation. Detailed computations of total head loss from the reservoir to the inlet of the storm conduit for a discharge of 90 cfs are presented in Fig. 2.19 and Table 2.2.

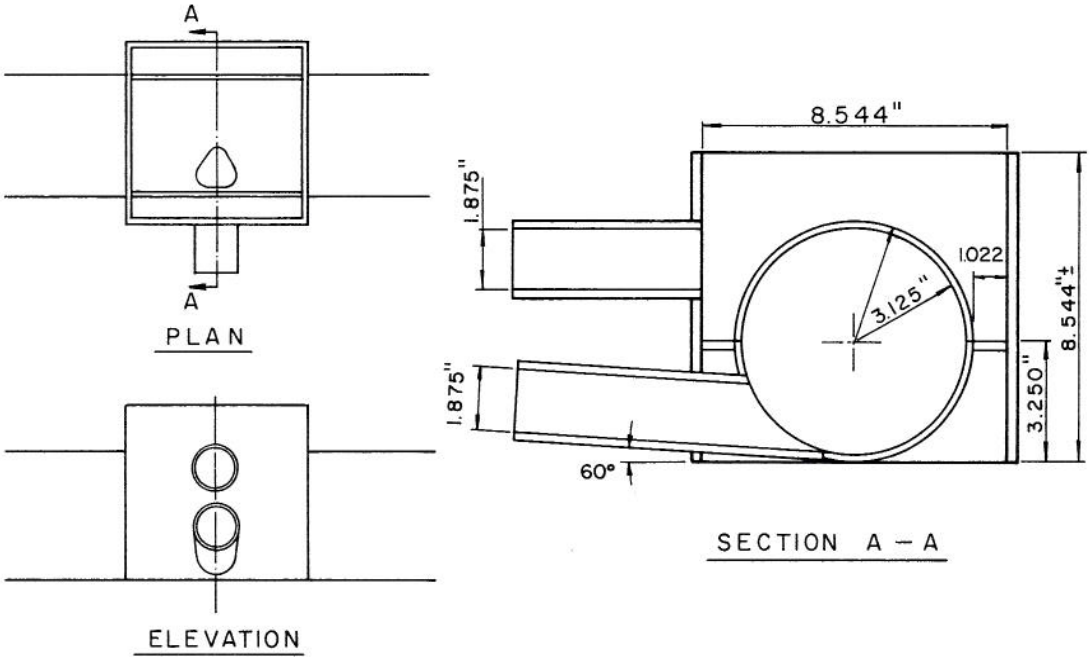

Fig. 2.10. Details of the junction box used in model study.

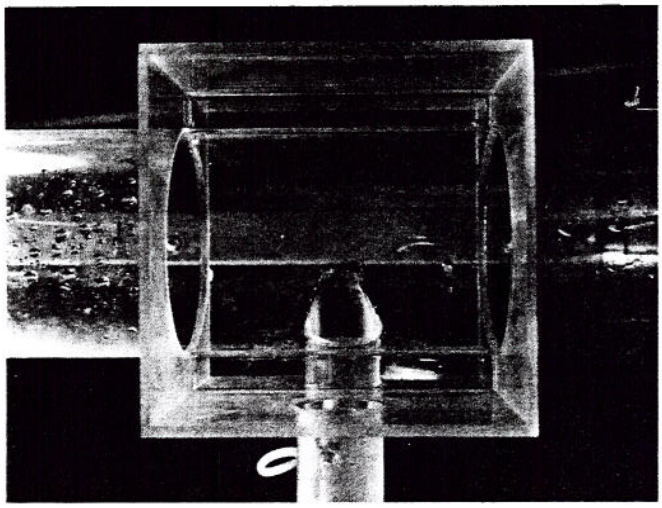

Fig. 2.11. Top view of the junction box used in the model study.

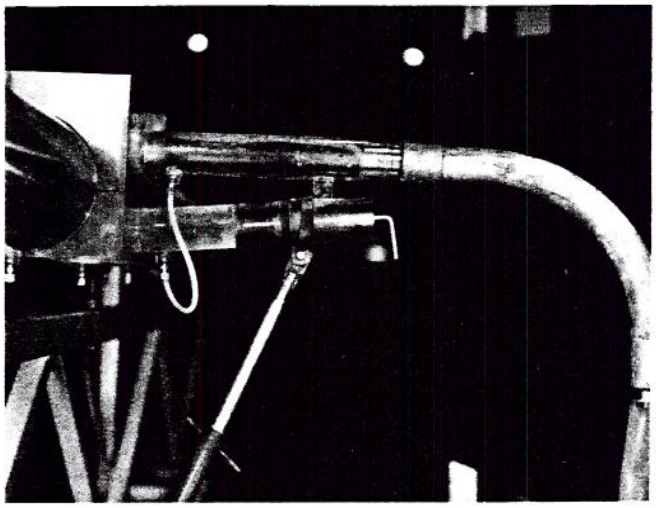

Fig. 2.12. The side view of the laterals and the junction box used in the model study.

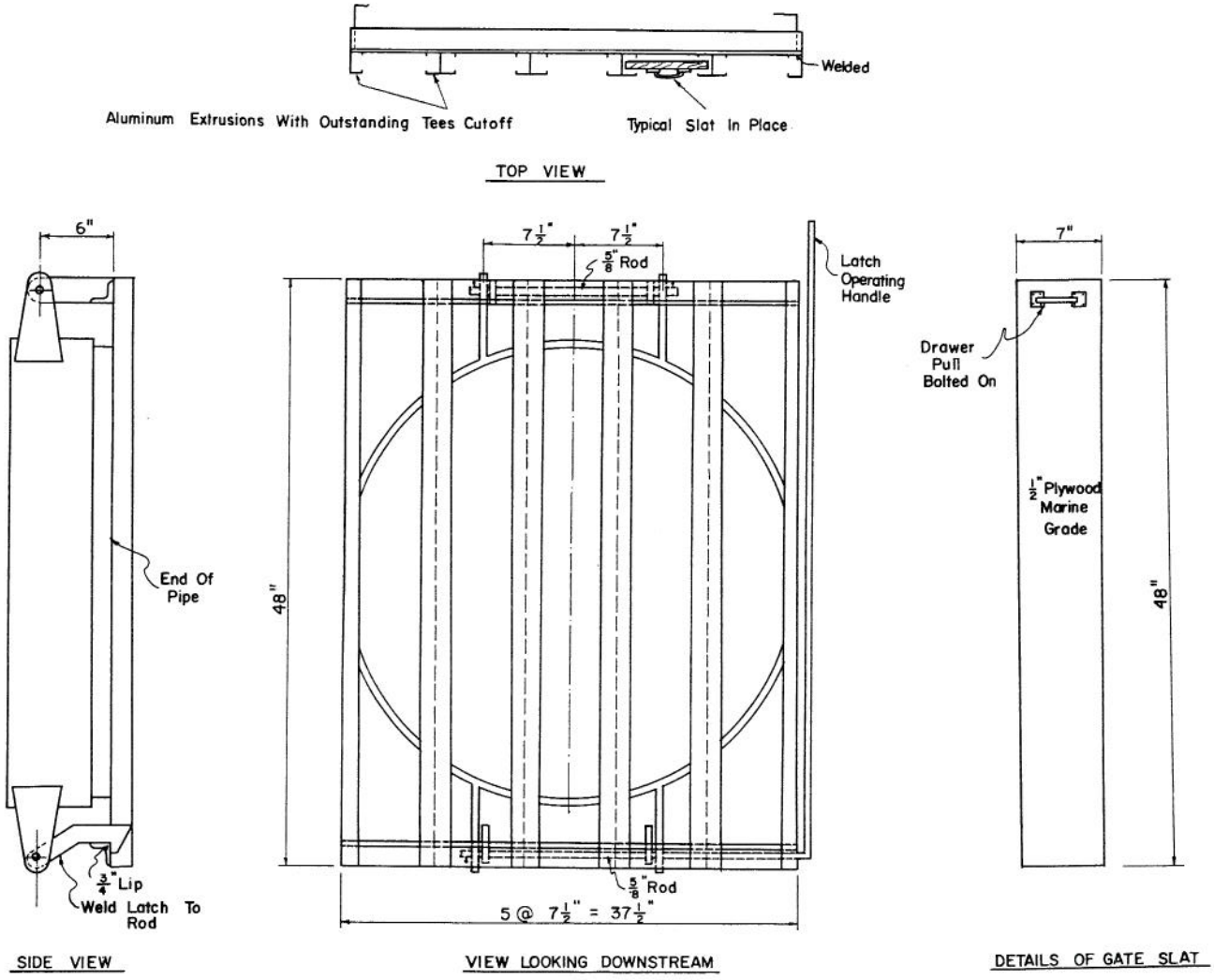

Fig. 2.13. Detailed dimensions of the outlet restriction gate.

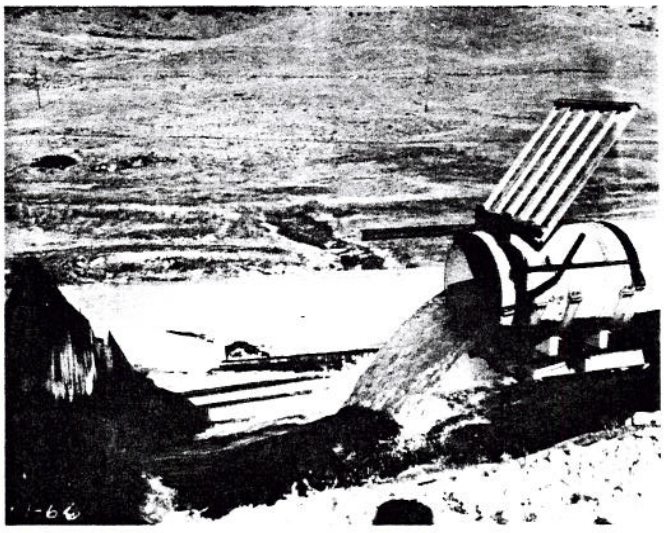

Fig. 2.14. The view of the removed outlet restriction gate for the conditions of a free outfall.

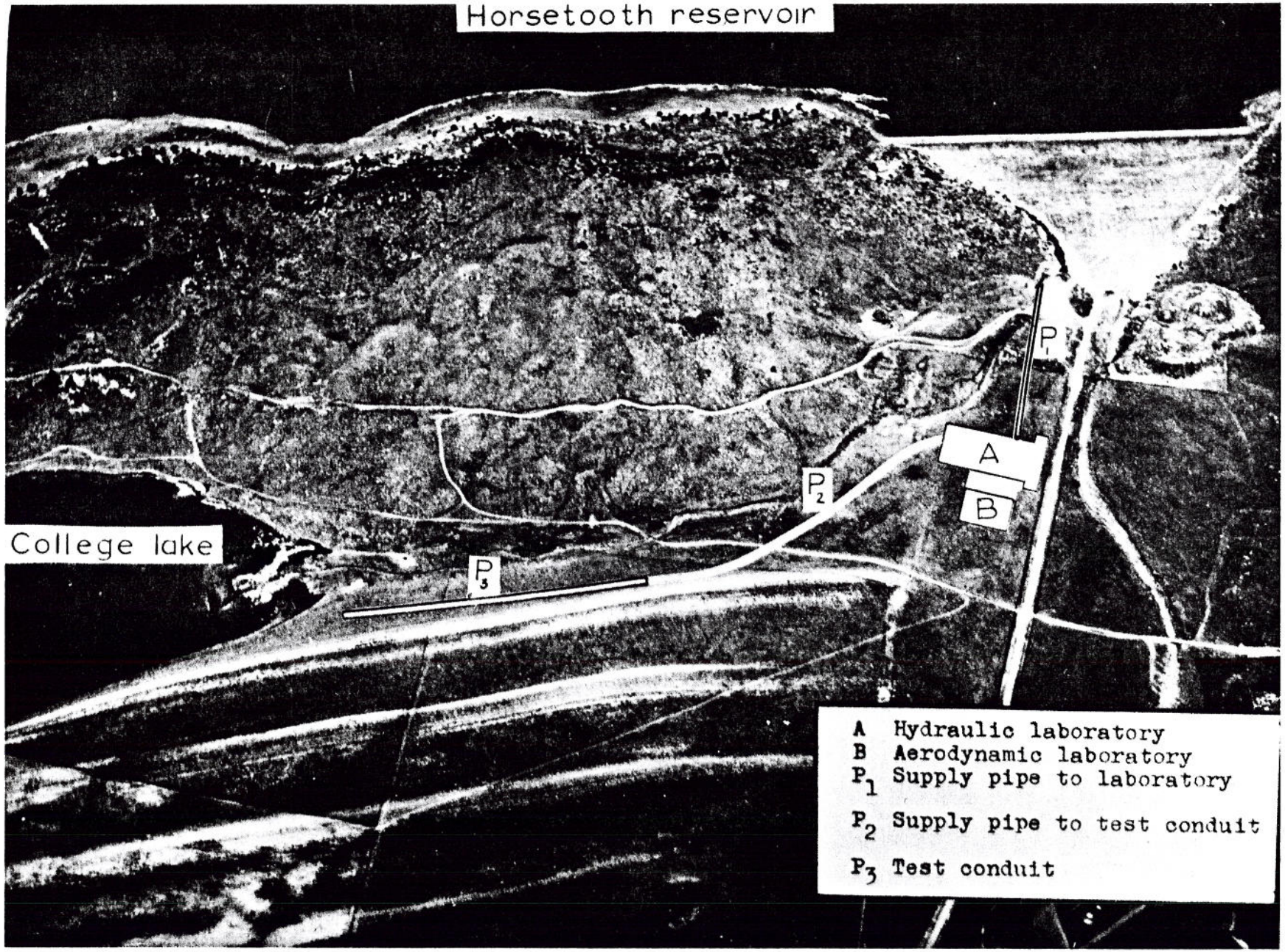

Fig. 2.15. General plan of the supply of water and of the storm conduit experimental facility location.

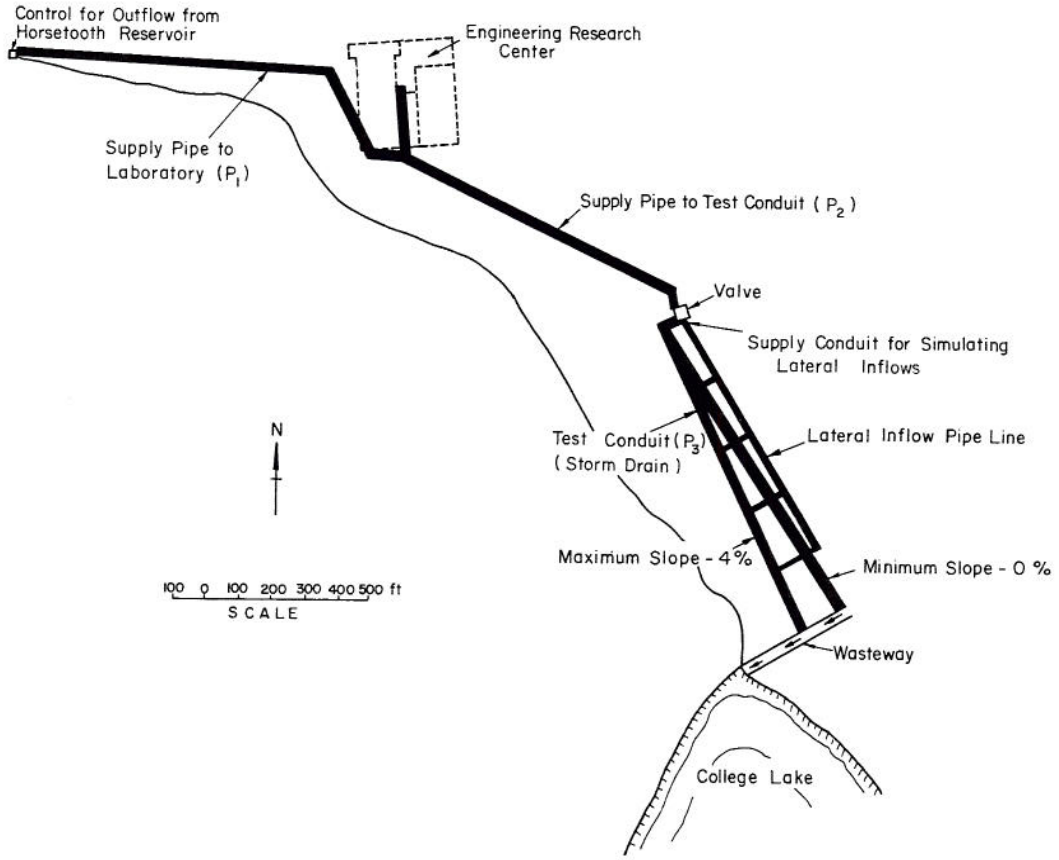

Fig. 2.16. General scheme for water supply and removal for storm conduit experimental facilities.

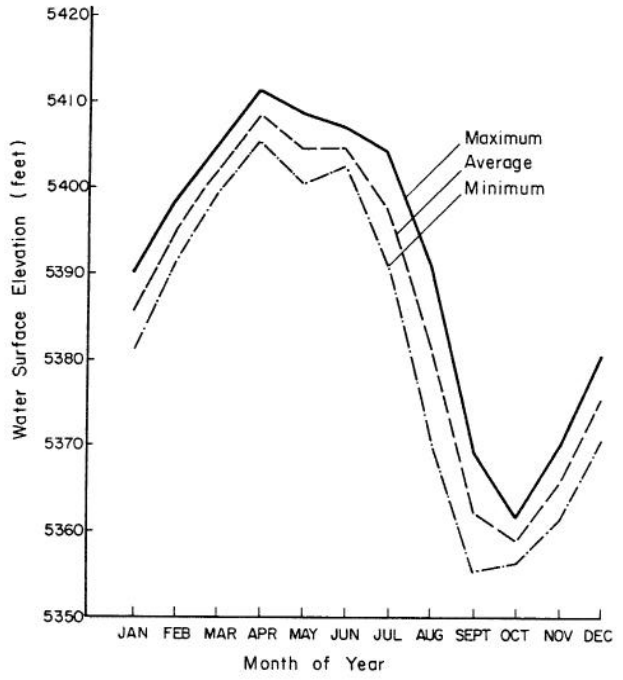

Fig. 2.17. Water level in Horsetooth Reservoir for period May 1951 ~ September 1962.

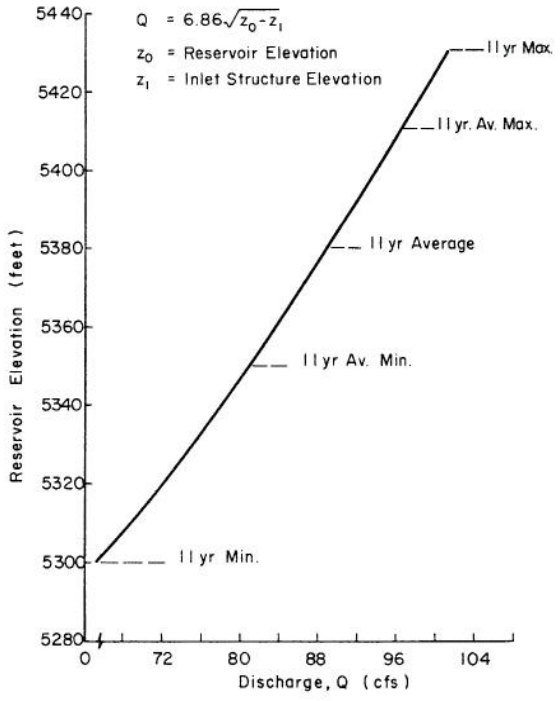

Fig. 2.18. Rating curve for discharge at the inlet structure of storm conduit.

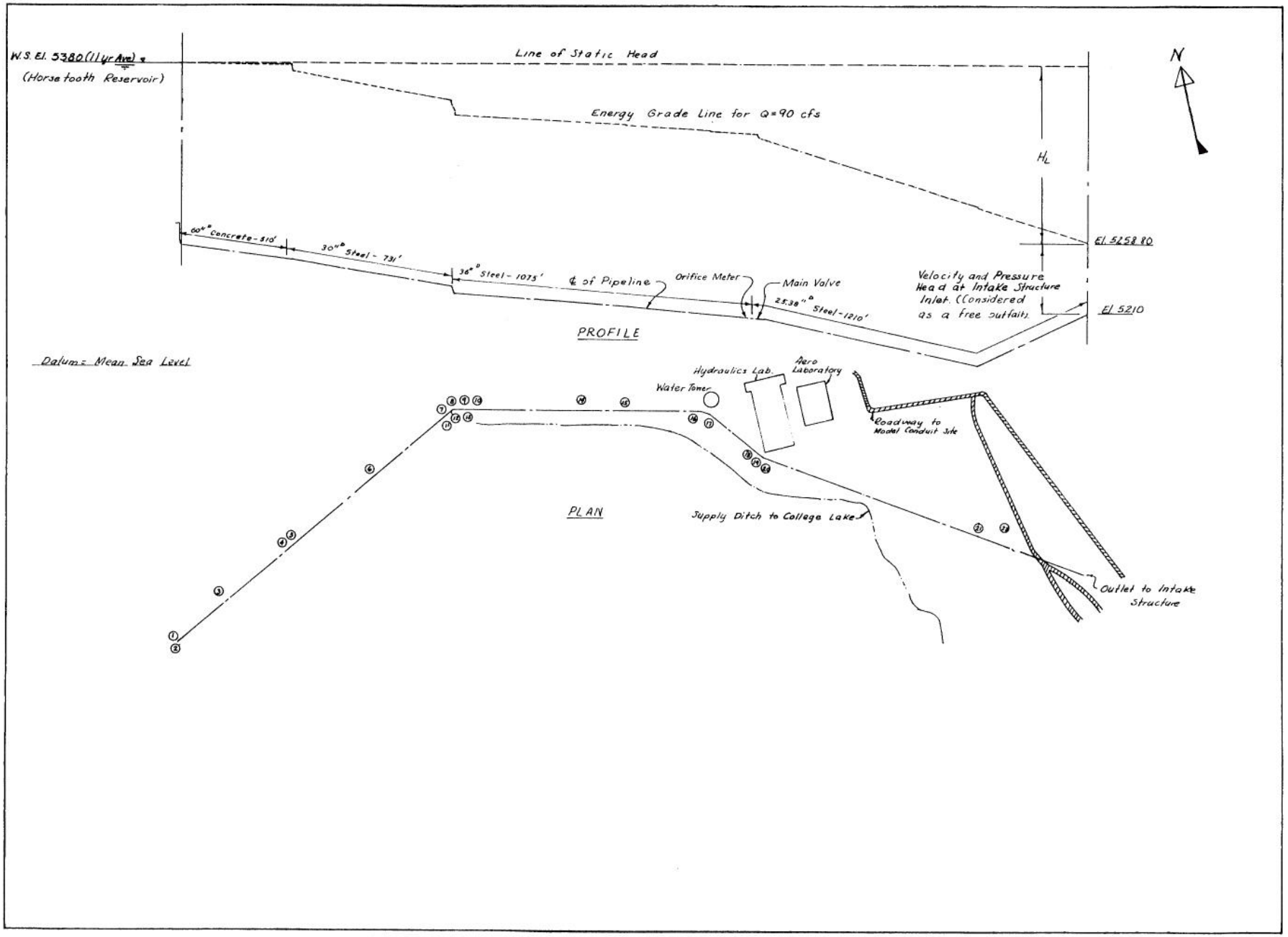

Fig. 2.19. Plan and elevation of supply line for the computation of head losses (numbers refer to pipe fittings of Table 2.2).

TABLE 2.2 Head losses in the supply line for storm conduit experimental facilities.

No.	Object	Station	Elevation, ft.	Loss Factor	Head Loss, ft.
1	Inlet	5+88.00	5270.00	0.50	0.163
2	Bend, 90°	5+91.00		0.13	0.042
3*	Friction			2.04	0.664
4	Contraction	10+90.00	5244.64	0.33	1.723
5	Valve	11+01.50	5244.64	0.25	3.186
6*	Friction			3.51	18.326
7	Wye	18+21.25	5227.00	0.30	1.566
8	Contraction	18+21.25	5227.00	0.04	0.510
9	Valve	18+29.75	5227.00	0.20	2.549
10	Bend, 45°	18+32.60	5227.00	0.12	1.529
11	Bend, 45°	18+37.11	5222.59	0.12	1.529
12	Expansion	18+37.56	5222.59	0.215	2.740
13	Bend, 40°	18+50.61	5222.39	0.08	0.201
14*	Friction			4.26	10.722
15	Wye	24+45.05	5213.27	0.30	0.755
16	Bend	26+83.75		0.10	0.252
17	Bend	27+13.75		0.10	0.252
18	Contraction	29+19.75	5205.59	0.04	0.408
19	Valve	29+29.75	5205.51	0.20	2.549
20	Bend	29+49.75	5205.52	0.10	1.020
21	T-Lateral	37+30.00	5173.65	0.03	0.306
22*	Friction			6.89	70.209
				TOTAL	121.201

W.S. Ref. Elevation 5380

*3 concrete 5 ft. D - 510 ft. L.
f = 0.02
*6 steel 2.5 ft D - 731 ft. L
f = 0.012
*14 steel 3 ft. D - 1075 ft. L
f = 0.012
*22 steel 25.38 in. D - 1210 ft. L
f = 0.012

Chapter 3

INSTRUMENTATION AND ITS CALIBRATION

3.1 Orifice Meters

Design of orifice plates. In order to provide sufficient flexibility to cover the expected range of flow rates, three sizes of sharp-edged circular orifice plates, based on the different orifice-to-pipe diameter ratios, were designed and used to measure the main inflow rate into the storm conduit. The ratios of the diameter of orifice to the diameter of pipe were 0.35, 0.50, and 0.70, respectively. They are referred to as small, medium, and large openings in the following descriptions.

The plates were made of stainless steel with thickness of 5/8 inches. Two sets of taps were used to measure pressure differentials. One set of taps was placed at one pipe-diameter (1D) upstream and the other set was placed at one-half pipe-diameter (D/2) downstream of the upstream face of the plate. For each set, eight taps spaced at 45 degrees were installed around the pipe wall and connected to a common manifold for measuring the average upstream and downstream orifice pressures.

Orifice calibration for steady flow conditions. The general orifice equation is

$$Q = C_d m A \sqrt{2gH} \quad , \tag{3.1}$$

in which C_d is the discharge coefficient, m is the ratio of the orifice area to the pipe cross-sectional area A, H is the differential head across the orifice, and Q is the discharge.

The purpose of calibration was to determine the discharge coefficient C_d by measuring H and Q for the known values m and A. The orifice plate was clamped between the flanges at a joint in a 26-inch diameter pipeline. The orifice plate was carefully adjusted so it was concentric with the pipe, and the pressure differential H was read from a differential manometer. A calibrated volumetric tank with a hook gage gave the volume of water for a measured period of time. Flow discharge Q was then obtained. The calibration equations obtained for the three orifice meters are:

1. For the small opening, with d/D = 0.35 and m = 0.1225,

$$Q = 2.102 \sqrt{H} \quad , \text{ with } C_d = 0.606 \quad . \tag{3.2}$$

2. For the medium opening, with d/D = 0.50 and m = 0.25,

$$Q = 4.439 \sqrt{H}, \text{ with } C_d = 0.627, \text{ and} \tag{3.3}$$

3. For the large opening, with d/D = 0.70 and m = 0.49,

$$Q = 9.783 \sqrt{H} \quad , \text{ with } C_d = 0.705 \quad . \tag{3.4}$$

Fig Figure 3.1 gives the relations between the three discharge coefficients and the Reynolds number for the small, medium, and large orifice openings, respectively. The three discharge coefficients were constant for the

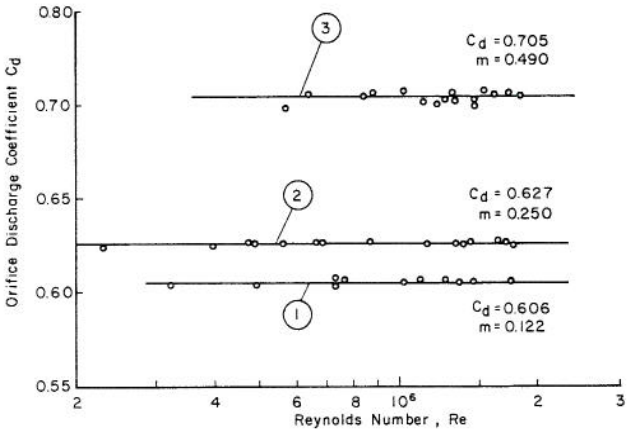

Fig. 3.1. Discharge coefficient C_d as function of the Reynolds Number, Re, of 36-inch O.D. pipeline for three orifice plates: (1) small (2) medium, and (3) large.

Reynolds numbers within the range 3.10^5 - 2.10^6 for the small opening, 2.10^5 - 2.10^6 for the medium opening, and 5.10^5 - 2.10^6 for the large opening. The Reynolds number in this case of orifice meters is defined by

$$R_e = \frac{Vd}{\nu} \quad , \tag{3.5}$$

in which V is the average flow velocity through the orifice cross-section, d is the diameter of the orifice, and ν is the kinematic viscosity of water. Temperature of water flowing through the conduit was almost constant, around 50°F, because the water supplied to the conduit system was taken from the bottom of the nearby Horsetooth Reservoir. The effect of the small changes of water temperature on the Reynolds number was hence negligible from one experiment to another. The error in C_d can be estimated by computing the deviations of the measured points from the constant values of C_d (solid lines in Fig. 3.1). The computed results are shown in Table 3.1.

TABLE 3.1. Errors in C_d of Fig. 3.1

Orifice	Standard Deviation	Relative Error (%)
Small	0.0041	0.5
Medium	0.0022	0.3
Large	0.0032	0.4

Unsteady flow considerations for orifice measurements. Before experimental tests were made, considerations were given to the problem of orifice calibration equation for the unsteady flow phenomenon of the wave passage through the orifice meter. It was assumed discrepancies may occur between the measurement of discharge in unsteady flow with a hydrograph configuration due to either acceleration or deceleration of the flowing fluid in comparison to the measurement of discharge in steady flow through the

orifice. The accelerating phase, or the rising limb of a hydrograph, would require increased pressure to produce acceleration of flow through the orifice meter. This increase of pressure would mean an increase of the pressure differential across the orifice meter. The use of this pressure difference to compute the steady flow discharge would give a greater value than the true flow would be for the pressure differential measured under the steady flow conditions. Similarly, the discharge of the decelerating phase, or the falling limb of the hydrograph, measured in a similar manner might indicate a smaller flow discharge in comparison to the discharge obtained for the pressure differential of the steady flow. It is expected, however, that the measured flow at the orifice meter for a complete hydrograph would be equal to the actual volume in steady flow because of the compensating effects of the accelerated and decelerated parts of the unsteady flow.

The order of magnitude of this error from the unsteadiness of flow under pressure is studied experimentally. If the discharge varied with time, the total volume can be measured directly by the calibrated volumetric tank. The calculated volume, W_c, for steady state conditions was computed by the numerical integration

$$W_c = \int_0^t Q_t dt \quad , \qquad (3.6)$$

in which the discharge Q_t is computed from the equation of the steady flow orifice, $Q_t = C\text{-steady} \cdot H^{\frac{1}{2}}$. In comparing the measured volume of the unsteady flow and the calculated volume of the steady-flow orifice equation, it was possible to infer whether the orifice coefficients, C, of the unsteady flow departed from the coefficients of the steady flow.

Experimental procedure also provided data for a comparison of the total measured volume of flow through the orifice plate under unsteady flow conditions for a given period of time, and the computed volume for the steady conditions by using Eqs. 3.2 through 3.4. The volumes of rising limbs, of falling limbs, and of the total hydrograph were measured directly by volumetric tanks while the pressure differential across the orifice plate was measured by a transducer and recorded on a strip chart. Within the limitations of the testing facility the runs were carried out in such a manner as to use almost maximum volumetric tank capacity while varying the times of runs and the peak flows.

Water was supplied to the test section containing the orifice plate by a pump. The unsteady flow condition was introduced by opening and closing a butterfly valve placed in the line specifically for that purpose. The valve, operated manually, was placed about 40 feet upstream from the orifice plate. A base flow was established. The water was diverted into the volumetric tanks, and the time of the run and the pressure differential across the orifice plate recorded. The diverter, time clock, and strip-chart were started at the same time the valve was opened or closed.

Volume of flow for steady condition over a given time was computed by numerical integration. Time intervals for the integration were taken as three seconds. At each three second interval on the strip chart recording, pressure was read and the flow rate computed using the steady flow orifice coefficient. The flow rate was averaged over the three second period and the volume for each time period determined and summed for the total. The actual computation was performed by digital computer.

Comparison of the direct measurement of volume to that computed from the transducer recorded data gave a maximum deviation of measured volume from the computed volume of 1.62 percent. Eleven of the sixteen runs or 69 percent of the runs gave deviations of measured volume from computed volume of less than one percent. No specific trend in the data was found. The results of comparing measured and computed volumes for various runs are shown in Table 3.2. Figure 3.2 shows the same results found in Table 3.2, which supports the conclusion that no significant deviation is observed because of unsteady flow conditions.

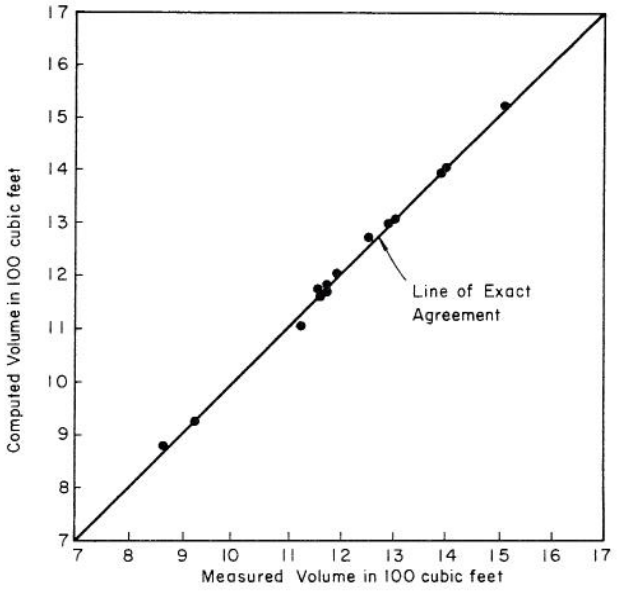

Fig. 3.2. Relation of the measured to the computed volumes for the unsteady flow conditions through the orifice meters.

In order to avoid surges of flow caused by a smaller orifice opening, 16 of the total 17 runs in Table 3.2 were made for the large orifice opening (m = 0.49) and only one run was made for the medium opening (m = 0.25). No data were taken for the small orifice opening (m = 0.1225).

3.2 Current Meters

Type of current meters. Propeller current meters have the following advantages as compared to cup current meters: (1) The propeller current meters produce smaller disturbances in flow, (2) The mechanical (bearing) friction is smaller in propeller current meters, and (3) The propeller current meters are less susceptible to fouling by foreign bodies carried in the flow. Based on these advantages, reliability of operation, and compact construction, the Ott propeller current meters with electric counters were selected to measure the flow velocities in the storm conduit. To cover a wide range of flow velocities, the Ott propeller current meters were equipped with interchangeable propellers with different pitches. The size and selection of the propellers and pitches are given in the Table 3.3.

TABLE 3.2. Results of unsteady flow investigation of orifice meter calibration for different area ratios

Run No.	Area Ratio	Hydrograph	Flow Rate cfs max	Flow Rate cfs min	Time of Test in sec.	Computed Volume in ft^3	Measured Volume in ft^3	Deviation of Computed From Measured Volume in %
3	0.49	Rising	23.704	12.111	62.99	1272.170	1252.091	-1.604
4	0.49	Rising	21.102	14.195	78.81	1408.636	1408.839	+0.015
5	0.49	Rising	22.100	9.439	59.95	1200.912	1193.531	-0.618
6	0.49	Rising	17.893	7.482	91.59	1317.455	1312.542	-0.374
7	0.49	Rising	22.261	10.053	62.25	1176.432	1160.429	-1.043
8	0.49	Rising	20.502	7.924	81.51	1397.028	1397.867	+0.060
9	0.49	Falling	21.585	6.584	59.48	1178.076	1173.244	-0.412
10	0.49	Falling	21.290	18.549	73.91	1524.571	1516.301	-0.545
11	0.49	Falling	21.290	15.265	65.07	1303.741	1297.380	-0.490
12	0.49	Falling	21.767	7.477	49.20	880.549	868.447	-1.394
13	0.49	Complete	22.188	6.765	62.61	1184.071	1173.726	-0.881
14	0.49	Complete	21.858	7.296	63.78	1107.155	1124.776	+1.567
15	0.49	Complete	22.351	8.132	61.37	1176.518	1168.864	-0.655
16	0.49	Complete	20.152	8.220	80.11	1174.248	1166.717	-0.645
17	0.25	Rising	17.041	8.305	60.07	924.271	923.561	-0.077
18	0.25	Rising	17.086	7.853	79.92	1155.196	1174.204	+1.619

TABLE 3.3. Selection of propellers

Propeller No.	Propeller Diameter (cm)	Pitch (cm)	Approx. Maximum Velocity (ft./sec)
2	5	10	3
2	3	10	3
3	5	25	8
4	5	50	16

To check the procedures used to determine the change, if any, in performance of the Ott current meters three series of tests were made using the Colorado State University calibration facilities (Figs. 3.3, 3.4, and 3.5).

In the first tests each meter propeller was tested singly. Each meter was mounted on a 3/8-inch rod attached to the carriage and towed at a depth of two feet (Fig. 3.3). The second test series involved three meters mounted on the 3/8-inch rod at a distance of 4-inches on centers. The purpose of the test was to determine interference effects, if any, on the meters operating under simulated field conditions. Because the recording system was only a single channel, it was not possible to record the performance of all three meters simultaneously. Therefore, the test procedure was the same for the single mounted meter, that is, it was necessary to make three runs with the carriage at a given speed in order to obtain the performance data at this speed on the three meters.

Since the velocities of the meters under field conditions fell on the uppermost range of a 3-range calibration chart plotted from data furnished by the Ott Laboratory, only the calibration data in this range were analyzed. In this range it was found that the theoretical curve that best fits the data is the asymptotic limb of a hyperbola, which can be approximated by a straight line of the form $V = a + bn$. In this equation V is the velocity in feet per second and n is the number of turns per second. Values of the coefficients a and b for least-square curves fitted to the recalibration data and the Ott laboratory data were found to be essentially identical. For each set of data the accuracy of the curve fitting procedure was found by the standard error of estimate of V on n.

In view of the general agreement between the recalibration values and the manufacturer's furnished values, there did not appear to be justification for the adoption of the recalibrated values. Furthermore, the effect of spacing the meters at 4-inches center to center does not indicate any trend when compared to the single meter calibration.

For the third test series a system was devised whereby all five velocity meters could be calibrated simultaneously utilizing the mounting arrangement used in the actual testing program of the storm conduit. A bracket was clamped to the front of the test car and the field mounting frame for the velocity meters was bolted to the bracket (Fig. 3.6). The velocity meters were tested at a depth of approximately one foot. A relay circuit operated by micro-switches provided means for turning a clock and the current meter counters on and off, (Fig. 3.7), while the test car traveled at constant speed over a known distance. Stakes were driven into the ground and cam plates were clamped to the stakes, (Fig. 3.8, lower right). Activation of the micro-switch was marked on the cam and the distance between the "on cam" and the "off cam" was measured. The tow car was initially at a point near the end of the water tank. During each run, the cams and micro-switches provided a time and count record over the known distance with variation being made only in time required to traverse the distance.

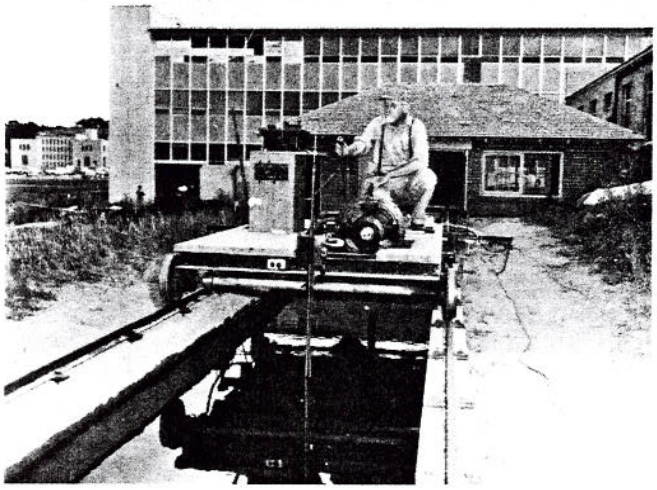

Fig. 3.3. Electrically propelled tow car.

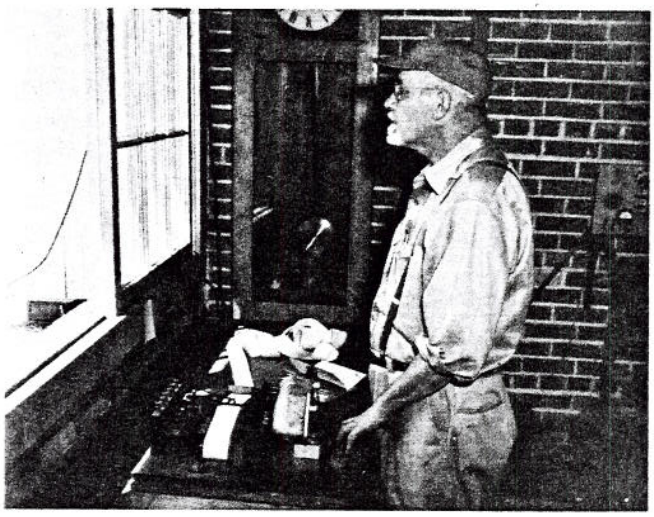

Fig. 3.5. Recording system for calibration of current meters, and tow car control switch. Strip chart records speed of tow car and revolutions per second of current meters.

Fig. 3.4. Current meter tow tank. Dimensions of the tank are: Length - 200 ft; width - 5 ft; depth - 5 ft.

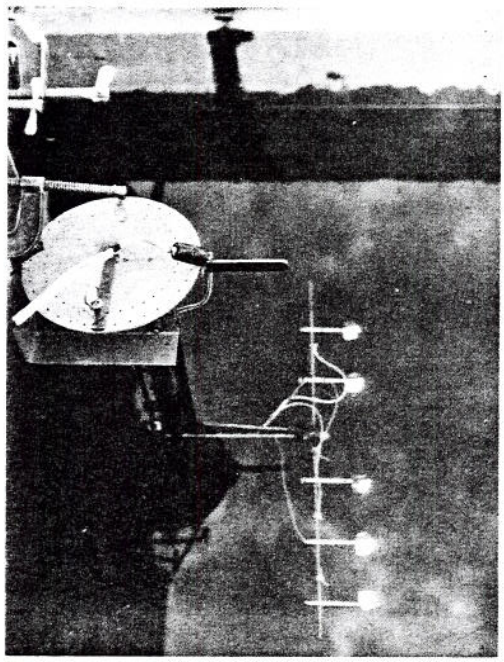

Fig. 3.6. Ott meters in calibration position on tow car.

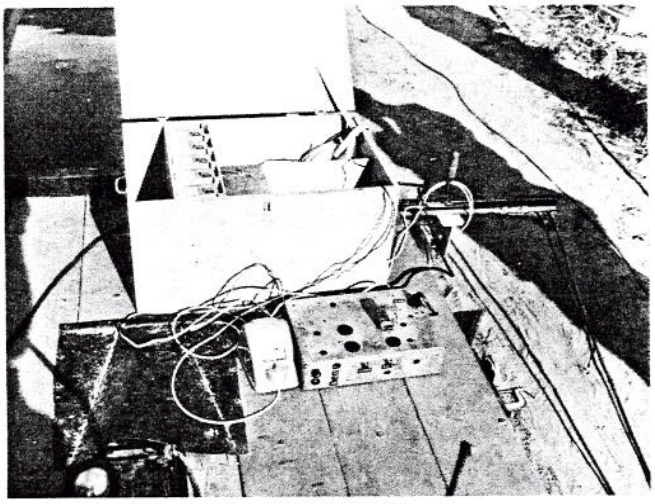

Fig. 3.7. Relay circuit chassis, electric clock, and current meter counters on tow car for simultaneous calibration of five Ott-current meters.

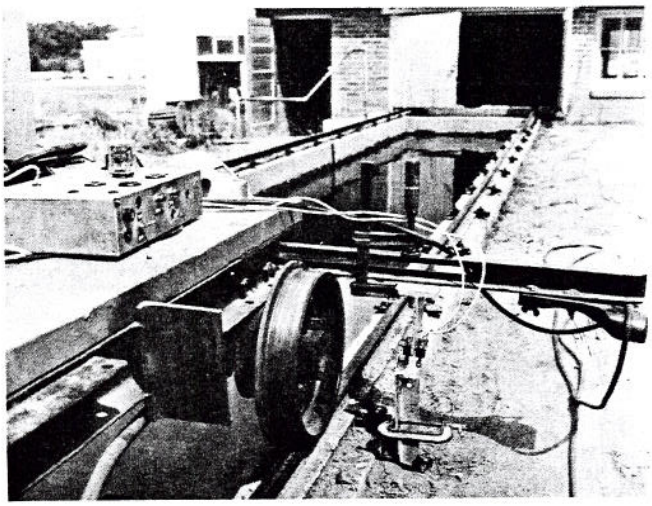

Fig. 3.8. Arrangement of micro-switch switches and cam plate which operate relay circuit. "Off cam" is illustrated.

Calibration results. The technique of calibrating the meters was found to be satisfactory, that is, the system was first carefully checked by making several runs of the tow car at a constant speed over a given distance until the meter count did not vary by more than ±0.5 percent. The meters were then calibrated by operating the tow car at eleven different speeds covering its operational range.

The calibration results of the values of "a" and "b" as compared to the original calibration data furnished by Ott Company are presented in Table 3.4.

Mutual interference and wall proximity effects on current meter readings. Investigations of mutual interference and wall proximity effects on current meter readings have been conducted by Henn [1], Status [2], Jovanovic [3], and Benini [3]. Based on the results of the tests of these investigators it was decided that similar tests would not be needed for the Ott current meters. Of particular importance were the results of the tests made by Benini, who was concerned with accurate measurement of flow in large diameter pipes. His calibration tests simulated the positioning of the current meters were similar to what were used by this study in the measurement of velocity distributions. Benini's rating equipment consisted of a flume 50.85 meters long (useful length between the two ends of the run 41.80 m), 2.00 meters wide and 3.00 meters deep; a carriage was operated by a cable system from a hydraulic converter enabling the required speed to be reached within a very short distance. The speed could be varied continuously between zero and 5.50 meters/second.

The experimental results obtained by Professor Benini are presented in Figs. 3.9 through 3.11. On the abscissa the axial distance between the propellers, or the distance between the propeller axis and the wall, is plotted in terms of the ratio between the distance L and the propeller diameter D. It was preferred to express the distance between the meter and the wall or between the two meters in terms of the propeller diameter rather than in absolute values, in order to extend the test results to meters with the propellers of different dimensions. The percentage deviations from the reference values are plotted as the ordinate. In Figs. 3.9 to 3.11 the representative points of the deviations have been joined by straight lines, to better emphasize the variation.

Apart from the tests carried out at the velocity of 0.5 meter/second, it can be seen that the divergences from the reference values are, with a single exception, less than 0.5 percent, and show no decisive trend in either the positive or the negative direction.

The tests reported thus demonstrate that within the range of velocities investigated the performance of a current meter is only slightly influenced by the proximity of a second current meter, or of a wall. The divergences found, referring to the behavior of meters in a region without any disturbances, are attributed rather to unavoidable experimental error, being of the same order of magnitude as, or slightly larger than, these errors. For this reason it is difficult to distinguish between experimental errors and effects caused by an adjacent meter or wall; it can be stated that, within the range investigated, the possible effect does not exceed 0.2 to 0.3 percent.

For comparison, the results of the other investigators are summarized as follows:

1. Staus [2] found that a propeller current meter records velocities that are low by 1.1 percent near the wall and by 0.8 percent when near the bottom, the errors being independent of absolute velocity.

2. Henn [1] made use of tests by the Ott firm. The Ott tests indicate that the reduction in current meter readings increases with the increasing velocity, to reach 1.2 percent for meters near the bottom and 2.1 percent for meters near the wall, at a velocity of 2.5 meter/second. Regarding the mutual interference of two nearby meters, the Ott tests indicate that in the velocity range 0.1 to 0.8 m/s, there is no significant correlation with the distance between the two meters.

3. Jovanovic [3] at the rating station at the Institute of Hydraulics in Belgrade found that in the velocity range of 0.5 to 4.5 m/s, meters near the bottom gave errors as large as 1.73 percent at a velocity of 4.5 m/s. Tests on meters placed 3 cm between the peripheries of the propellers gave errors of only 0.8 percent at 4 m/s.

TABLE 3.4. Comparison of Ott-Meter calibration rating curves, V = a + b n, by the least square estimate of Ott and CSU calibration data for meter velocity > 1.0 fps.

Meter No.	Prop. No.	Prop. Dia. cm.	Slope of curve b	Intercept a	Standard Deviation σ	Calibration Date	Remarks
12457	2-3	3	0.3411	0.108			From mfg.[1] calibration curve for meter.
			0.338	0.143	0.0016	5-1-64	1st test series; single meter.
			0.339	0.106	0.0051	7-2-64	2nd test series-run 1; deepest of 3 meters.
			0.337	0.111	0.0059	7-13-64	2nd test series-run 2; deepest of 3 meters.
			0.340	0.112	0.0042	7-15-64	From analysis of original data.*
12457	4	5	1.6531	0.030			From mfg. calibration curve for meter.
			1.675	-0.007	0.0074	5-1-64	1st test series; single meter.
			1.648	0.049	0.0078	7-2-64	2nd test series-run 1; deepest of 3 meters.
			1.648	0.029	0.0074	7-13-64	2nd test series-run 2; deepest of 3 meters.
			1.651	0.036	0.0052	7-15-64	From analysis of original data.
			1.693	0.007	0.0429	8-24-64	3rd test series; meter mounted on field support with original meter gear replaced by a new gear.
12458	2-3	3	0.3395	0.115			From mfg. calibration curve for meter.
			0.335	0.177	0.0059	5-1-64	1st test series; single meter.
			0.336	0.153	0.0034	7-2-64	2nd test series-run 1; middle meter of 3.
			0.338	0.124	0.0019	7-13-64	2nd test series-run 2; middle meter of 3.
			0.338	0.131	0.0056	7-15-64	From analysis of original data.*
12458	4	5	1.6531	0.033			From mfg. calibration curve for meter.
			1.651	0.016	0.0104	7-2-64	2nd test series-run 1; middle meter of 3.
			1.663	0.018	0.0135	7-13-64	2nd test series-run 2; single meter of 3.
			1.642	0.051	0.0088	7-13-64	2nd test series-run 3; middle meter.
			1.650	0.040	0.0098	7-16-64	From analysis of original data.*
			1.673	-0.001	0.0385	8-24-64	3rd test series; meter mounted on field support with original meter gear replaced by a new gear.
12459	2-3**	3	0.3395	0.112			From mfg. calibration curve for meter.
			0.339	0.150	0.0050	5-1-64	1st test series; single meter.
			0.342	0.122	0.0109	7-2-64	2nd test series-run 1; shallowest of 3 meters.
			0.340	0.112	0.0141	7-2-64	2nd test series-run 2; shallowest of 3 meters.
			0.341	0.115	0.0055	7-13-64	2nd test series-run 3; shallowest of 3 meters.
12459	4	5	1.6564	0.036			From mfg. calibration curve for meter.
			1.675	0.027	0.0099	5-1-64	1st test series; single meter.
			1.668	0.022	0.0101	7-2-64	2nd test series-run 1; shallowest of 3 meters.
			1.681	0.007	0.0093	7-2-64	2nd test series; single meter.***
			1.668	0.017	0.0176	7-13-64	2nd test series-run 2; shallowest of 3 meters.
			1.654	0.043	0.0053	7-17-64	From analysis of original data*.
			1.691	0.004	0.0451	8-24-64	3rd test series; meter mounted on field support with original meter gear replaced by a new gear.

[1]Mfg. means manufacturer's calibration results.

TABLE 3.4. Comparison of Ott-Meter calibration rating curves, $V = a + b\,n$, by the least square estimate of Ott and CSU calibration data for meter velocity > 1.0 fps. - Continued.

Meter No.	Prop. No.	Prop. Dia. cm.	Slope of curve b	Intercept a	Standard Deviation σ	Calibration Date	Remarks
12460	2-3	3	0.3362	0.118			From mfg. calibration curve for meter.
			0.334	0.156	0.0027	5-1-64	1st test series; single meter.
			0.335	0.127	0.0042	7-17-64	From analysis of original data*
12460	4	5	1.6466	0.033			From mfg. calibration curve for meter.
			1.666	0.023	0.0171	5-1-64	1st test series; single meter.
			1.643	0.044	0.0063	7-18-64	From analysis of original data.*
			1.700	-0.032	0.0397	8-24-64	3rd test series; meter mounted on field support with original meter gear replaced by a new gear.
12461	2-3	3	0.3378	0.112			From mfg. calibration curve for meters.
			0.333	0.156	0.0050	5-1-64	1st test series; single meter.
			0.338	0.109	0.0035	7-9-64	From analysis of original data.*
12461	4	5	1.6498	0.030			From mfg. calibration curve for meter.
			1.670	-0.008	0.0078	5-1-64	1st test series; single meter.
			1.652	0.024	0.0041	7-19-64	From analysis of original data.*
			1.674	-0.019	0.0378	8-24-64	3rd test series; meter mounted on field support with original meter gear replaced by a new gear.

* Original calibration data furnished by Ott Company. Note: This data was used in preparation of the calibration curve supplied by Ott with each meter.

** No original data was furnished for this propellor.

*** Meter shaft had been bent during operation; calibration was made after meter was required.

These results are at variance with those by Benini. Because of the different technique used by Benini in carrying out the tests, in particular by comparing calibration tests carried out successively with repeated tests, the results given by Figs. 3.9 to 3.10 are liable to less error and are therefore assumed to be reliable.

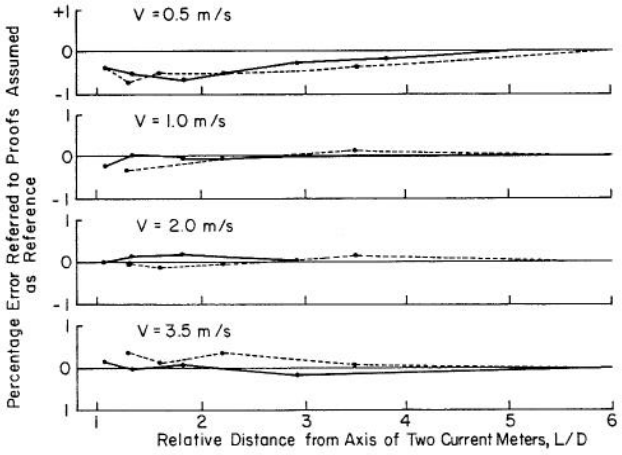

Fig. 3.9. Behavior of two neighboring current meters with propellers of different pitch (after Benini).

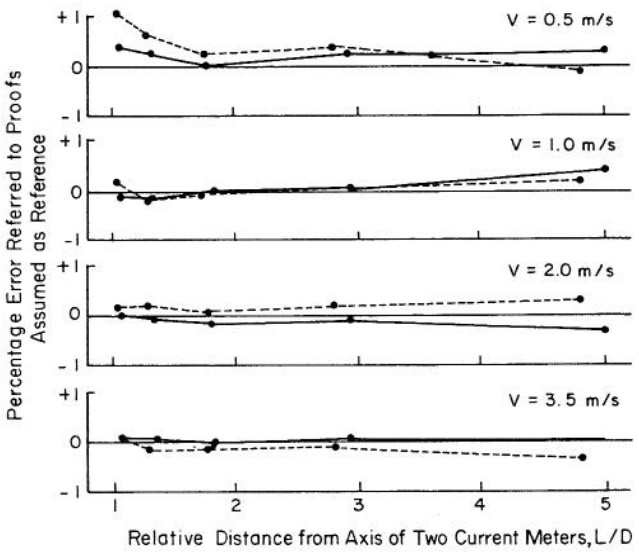

Fig. 3.10. Behavior of two neighboring current meters with propellers of the same pitch (after Benini).

In summary, since mutual interference and wall proximity effects on current meter readings are negligible in the velocity range of this project's

experimental studies, it was decided that a particular calibration of the current meters for these effects should not be made. Instead, the German code for the meter use was adopted. The code specifies that the distance between the meter axis and the wall must not be less than 0.75 times the diameter, and the distance between the two adjacent meters must be less than 1.2 times the propeller diameter.

3.3 Pressure Transducers

General considerations. The calibration of pressure transducers is considered from those standpoints: (a) that the output voltage be zero for zero pressure input; (b) that the output voltage be a linear function of the input pressure differential; (c) that it does not change with time and if so, it must be systematically checked, and (d) that the proportionality constant between the input and the output be known before the observed data can be interpreted.

The proportionality constant may be reasonably expected to include the composite effects of all elements in the data recording system. Hence, this constant should be established immediately prior to and immediately following data observation. It was not assumed this value would remain constant from run to run or from day to day, so facilities were implemented to determine this value in the field as desired without making a complete calibration check, which essentially only establishes the linearity of the transducer.

The first, second and third conditions under (a), (b), and (c) have been investigated for all transducers in use. With sufficient care in installation and adequate warm-up time, all transducers were linear and passed through zero with no hysteresis for the range of pressure differentials anticipated measurements. The manufacturer's specifications state a compensated temperature interval of these pressure transducers ranges from -65°F to +250°F. During the tests, the air temperature was 75° ± 10°F, and the water temperature was almost constant, around 50°F. It is thus concluded that the temperature effect on the pressure transducer measurements was negligible.

Procedures of calibration and results. A 3-foot water manometer was used to give the differential depth in conjunction with the pressure transducer. The readout part of the pressure transducer was provided by a digital voltmeter. For each test, the adjustment of zero pressure to zero voltage output was made. The difference of water levels of the manometer with corresponding voltage output from the pressure transducer were then recorded. The plots of digital readout in volts versus the difference of water levels in feet were used to check the linearity of the pressure transducers. The calibration results of different pressure transducers are shown in Figs. 3.11 and 3.12.

3.4 Pitot Tubes

Early in the investigation of velocity distributions a single pitot tube was considered. A particular tube was calibrated and used for one vertical velocity traverse. Its calibration constant was essentially 1.00 for relatively small velocities. There was a slight difference in the velocity profile as observed by the pitot tube and the Ott current meters for the same flow conditions, but because of the time involved in using a single tube to define the complete velocity profile and because the Ott current

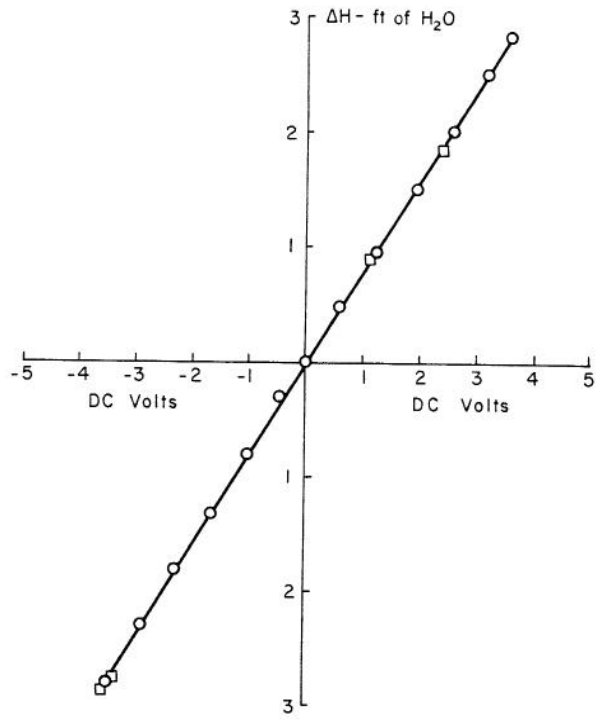

Fig. 3.11. The calibration line for the pressure transducer No. 12180, ± 1 psi.
Tested 7-23-66
Using data recording system.
CD-25 No. 14490

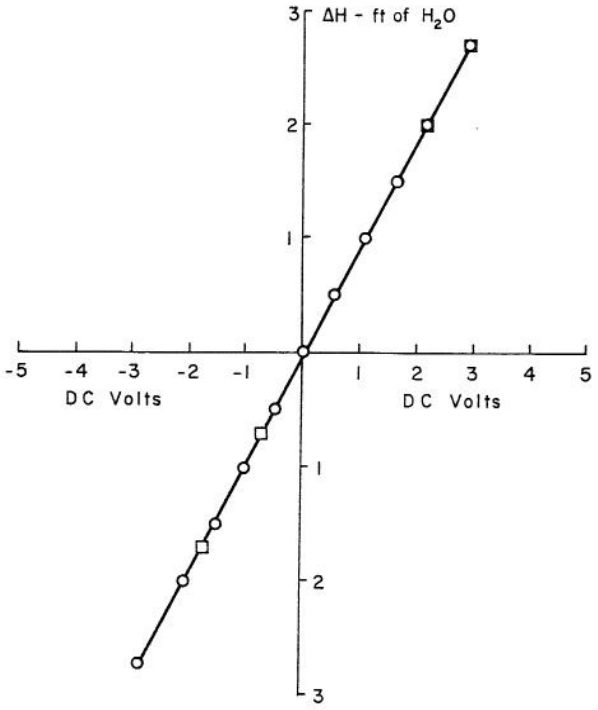

Fig. 3.12. The calibration line for the pressure transducer No. 14400, ± 5 psi,
Tested 7-23-66
Using data recording system.
CD-25 No. 17083

meters produced essentially the same vertical profile with a fraction of the time requirement, the use of the single tube was discontinued.

Velocities in excess of 10 feet per second, for the steeper slopes, reduce the use of the Ott current meters. In order to reduce field run times to a minimum and to reduce the drag on the velocity meters and accompanying support to a minimum, hypodermic needles (as shown in Fig. 3.13) were used to measure the total static and dynamic head. The static head was measured at the solid boundary surface. Seven of these were arranged along a revolving radial arm. Based on the use of similar tubes in air flow at high Reynolds numbers the coefficient was assumed to be constant for the range of velocities being observed. Considering this assumption and the fact that if the distribution of velocities as represented in the α and β velocity distribution coefficients only was desired, then these coefficients can be represented by the appropriate integral of the ratio of the square root of the pressure differential. The pressure differentials were detected by means of a pressure transducer whose voltage output was proportional to the pressure differential. The voltage was read and recorded automatically onto punched cards. Since the voltage was proportional to the pressure differential, the velocity distribution is identical to the distribution of the square root of the observed voltages.

Subsequent comparison of velocity distribution coefficients as measured by the Ott current meters and by the hypodermic dynamic tubes indicated an overlap within the ranges of variability of the Ott meter results. Therefore, it did not appear desirable or necessary to calibrate the dynamic tubes for the determination of the velocity distribution coefficients.

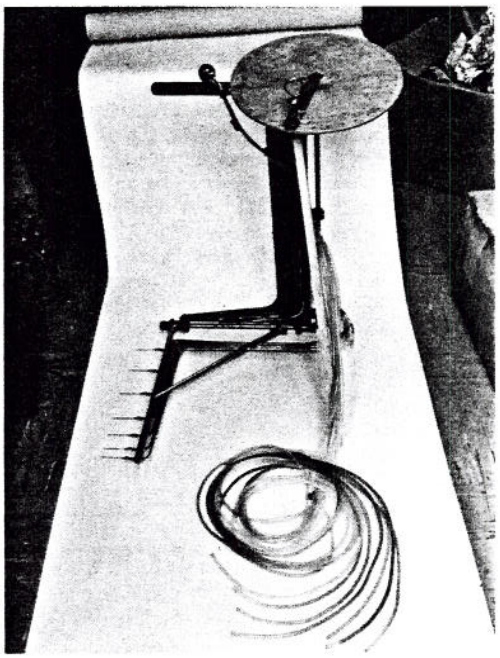

Fig. 3.13. Pitot tube rake used for point velocity measurements at large discharges of supercritical flow.

Chapter 4

DATA RECORDING SYSTEM

4.1 Description of the System

A system for recording and transmitting field data from the outdoor storm conduit was installed. The continuous time series of physical quantities measured by the sensing device were first transferred into analog electric signals and were then digitized by an analog-to-digital converter. The output from the analog-to-digital converter in the form of punched cards or tapes were then fed into computer for further computations. Figure 4.1 shows the general outline of the Data Recording System.

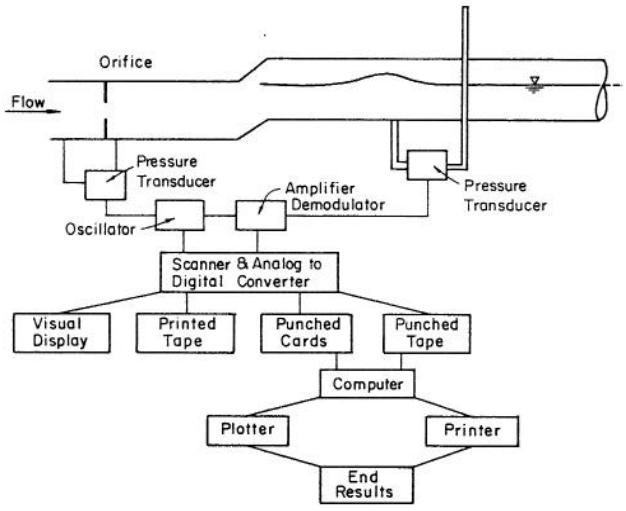

Fig. 4.1. Data recording system.

4.2 Analog-to-Digital Converter

The Systron-Donner Model 1234 Analog-to-Digital (A/D) converter was designed to accept continuous (analog) data up to 30 input channels. It sequentially scans, digitizes, and drives an output coupler to punched cards or punched paper tapes for eventual computer processing. The system samples at a rate determined by the type of output device and the number of digits per word. For punched cards, the rate is 2 words or 17 characters per second. For punched paper tape, it is 14 words or 110 characters per second. A pinboard provides the means of setting the full-scale input range of each channel to be scanned. These ranges are ±10, 50, 100, and 500 millivolts, 1, and 10 volts. The same pinboard allows any unused or unwanted channels to be deleted from the scan. Each sample is of 3 milliseconds (ms) duration and the next sample is taken T milliseconds later, (Fig. 4.2). The T is determined by the time required for digitizing, punching, etc; however, its duration may be varied by choice of output device and number of characters printed out per sample. For a standard 8-digit data word, with card punch output, T is 500 ms less 60 ms/digit deleted. With paper tape output, T is 70 ms less 9 ms/digit deleted.

The output from the A/D converter of "time" and "manual data" are printed out at the beginning of each scan though they could be omitted at the option of the operator.

The following is printed out for each channel:

Channel identification	2	digits
Polarity or overload	1	"
Data	4	"
Range or data ID	1	"

Q is printed out for an overload.

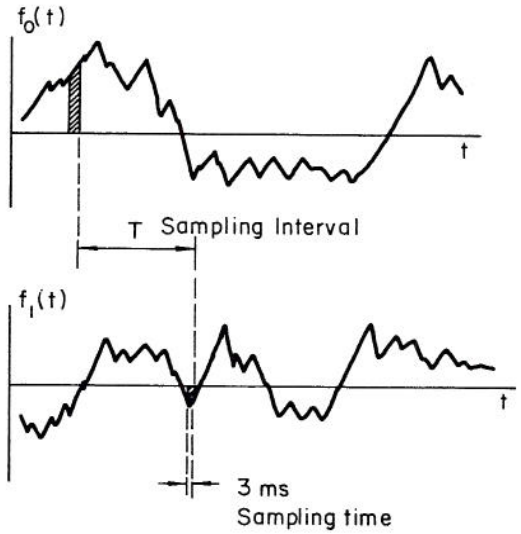

Fig. 4.2. Schematic representation of time series sampled by data recording system.

At the option of the operator the system may enter six digits of time information at the beginning of each record (scan). The indication and recording of time is in hours, minutes, and seconds. The source of each input data point is identified by a two digit channel number preceding the value of the data taken. Each four digit value is accompanied by indicators for range, polarity, and "off-scale" conditions.

The range symbol is:

volts full scale	Symbol
10 "	3
1 "	4
0.5 "	1
0.1 "	5
0.05 "	2
0.01 "	6

For the decade steps, the range symbol is the negative power of 10 by which the data is to be multiplied. The number 8 identifies the data as a manual entry and the number 9 identifies a time entry. For example,

05-74973 means that a value of -7.497 is read for channel 5,

14+53922 means that a value of +0.02696 is read for channel 14,

24Q10733 means that channel 24 is overloaded,

13+45329 means a time of 13 hours 45 minutes 32 seconds, etc.

The details of the data format as the output from the A/D converter is 0.1% at full scale.

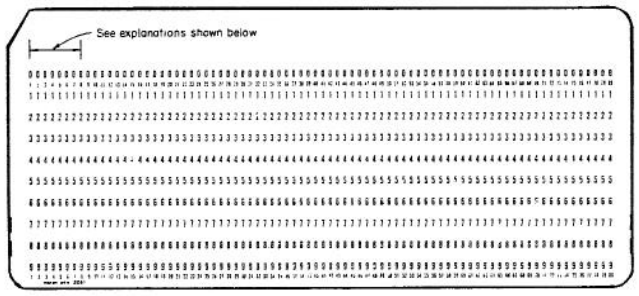

	Columns (1-8)								
	1	2	3	4	5	6	7	8	1-500μV 2-50 μV 3-10 V 4- 1 V 5-100μV 6-10 μV
Voltage	c	c	±	v	v	v	v	R	
	channel number		sign						
Time	H	H	+	M	M	S	S	9	
	Hours			Minutes		Seconds			
Identification	I	I	-	I	I	I	I	8	

Fig. 4.3. The data format as the output from Analog-to-Digital Converter.

4.3 Operations and Controls

The outdoor circular storm conduit is located about 1500 feet away from the Colorado State University Hydraulic Laboratory building. Data taken from the storm drain were transformed into electric voltage signals by the pressure transducers installed in the control trailer, shown in Fig. 4.4. The transducer's slope and intercept calibrations for head versus voltage relations were determined in the following manner. First, the systems were allowed to come to equilibrium. The zero transducer voltage output was then recorded. Next, valves No. 1 and No. 3 were closed and a differential head was applied in manometer tube A. This was measured and recorded along with the corresponding transducer voltage output. Once these calibrations were obtained, all valves were opened and the systems were again allowed to return to equilibrium. Then valves 2 and 3 were closed and the wave was started. Using this system, the deviations from the initial depths were recorded.

Flow passed through a motor-driven Rockwell Permisphere valve, then through an orifice where a constantly recording pressure transducer was connected to measure discharges. It then passed through a baffle system to dampen out surface oscillations and provide a more uniform velocity distribution, and, finally, on to what is considered the inlet of the pipe.

Waves were measured at distances of 50.00 ft, 410.00 ft, and 771.70 ft from the entrance during experiments of the summer of 1965 and at distances of 50.00 ft, 251.24 ft, 387.70 ft, 462.56 ft, 669.83 ft, and 771.70 ft during experiments of the summer of 1966. Wave heights were measured by pressure transducers connected between the pipe invert and a set of manometers, as shown in Fig. 4.4.

Voltage signals were converted from analog to digital form in the data recording system and were then punched directly onto data cards. The experimental wave could then be reconstructed by feeding the calibration and voltage cards into a digital computer which converted the voltages into depths.

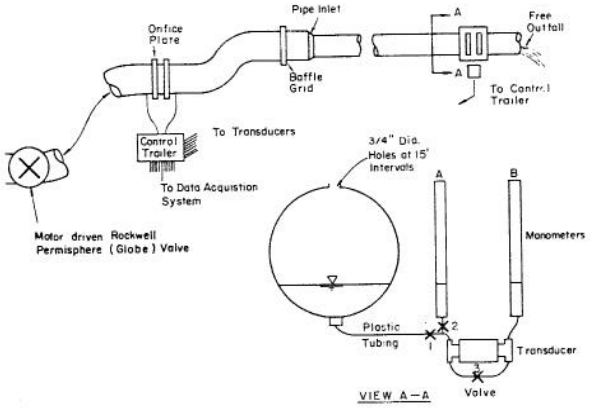

Fig. 4.4. Schematic representation of facilities and data recording system.

Chapter 5

EXPERIMENTAL TEST CONDITIONS AND TYPICAL RESULTS

5.1 Steady Flow Conditions

Cross-sectional velocity distributions. In order to determine the velocity distribution coefficients (α and β) experimentally, measurements of the distribution of conduit cross-sectional velocities were made. Time average point velocities were measured by the Ott laboratory current meter. Five meters were mounted on a rod which was supported at the center. The rod support was at the conduit centerline and could rotate to place the meters in any angular position. The meters were spaced along the rod to sample equal circumferential areas. The meters were placed at the minimum recommended spacing distance from the conduit wall. The meter support rod was positioned at angular intervals of 10 degrees. Thus, the point velocities were observed at five radial positions and as many 10-degree intervals as required to sample the circular segment.

The input data to the computer program consisted of: (1) velocity meter identification number and propeller number; (2) velocity meter position on rod, (3) angular position of the rod, (4) time interval of revolutions, (5) number of revolutions, (6) water depth at the cross-section, and (7) measured discharge.

A typical result of the measured velocity distributions of the conduit cross-section is shown in Fig. 5.1. The properties and computation details of these velocity distribution coefficients, α and β, based on the measured velocities of conduit cross-sections are described in Part III of this four-part series of papers. This paper is the second in the series.

Boundary roughness. The conduit boundary roughness was determined from experimental observations. In this approach the Darcy-Weisbach friction factor f and the conduit Reynolds number Re were computed from measured depths and discharge.

Hook gage readings, gage zeros, and conduit invert elevations were measured at the successive piezometer locations shown in Table 5.1 The discharge was determined from the calibrated orifice meters. By knowing the depths and discharges for fixed conduit invert slopes, the average velocities and the total energy heads were then computed. The difference in successive values of total energy heads divided by the distance between conduit stations represents the energy loss rate. This loss rate and the average hydraulic radius were substituted into the resistance equation to evaluate the friction factor f, namely

$$f = \frac{4 R_{av}}{\frac{V_{av}^2}{2g}} \cdot \frac{\Delta E}{\Delta x} \quad . \qquad (5.1)$$

The Reynolds number for the same reach was computed, based on average velocity and hydraulic radius as the characteristic length, i.e.

$$Re = \frac{V_{av} \cdot R_{av}}{\nu} \quad . \qquad (5.2)$$

A plot of these f values versus Reynolds number, Re, are presented in Fig. 5.2. The plotted points represent the results of experimental ranges of depth from 0.56 to 2.6 feet or depth-to-diameter ratios of 0.19 to 0.89. The discharges varied from 2.25 to 72.0 cfs. The corresponding Reynolds number range is from approximately 3×10^4 to 1×10^6.

TABLE 5.1. Piezometer locations

No.	Distance from upstream end	Incremental Distances
1	20.00	
2	100.00	80.00
3	197.00	97.00
4	308.40	111.40
5	406.10	97.70
6	509.60	103.50
7	613.20	105.60
8	707.20	94.00
9	772.20	65.00
10	802.20	30.00
11	807.25	5.05
12	812.25	5.00
13	816.25	4.00
14	819.10	3.00
15	820.70	1.60
16	821.70	1.00

Controlled and free outfall. The mathematical simulation of the downstream boundary condition for the controlled outflow required the calibration of a terminal (end) restriction. Any geometric configuration was acceptable if it satisfied certain criteria:

1. The discharge as a function of depth could be expressed simply, such as $Q = my^n$ in which m and n are constants and y is the depth of flow upstream of the restrictions.

2. The restriction was not so great as to cause the pipe to flow full under the maximum anticipated hydrograph discharge.

3. The approach-velocity distribution was symmetrical and did not differ appreciably from the undisturbed flow.

These criteria were satisfied by a restriction gate consisting of five 7-inch vertical wooden slats held in position by 2 1/2-inch wide vertical aluminum H-sections. The clear opening was five inches between supports. The discharge could thus be controlled by varying the vertical position or by removing one or more slats (Figs. 2.13 and 2.14).

Calibration of various combinations of openings was made by measuring the corresponding discharge and the water surface elevation approximately 20 feet upstream of the control. For the range of discharges anticipated in the unsteady flow runs, it was concluded that the best combinations of openings was with the center three slats removed.

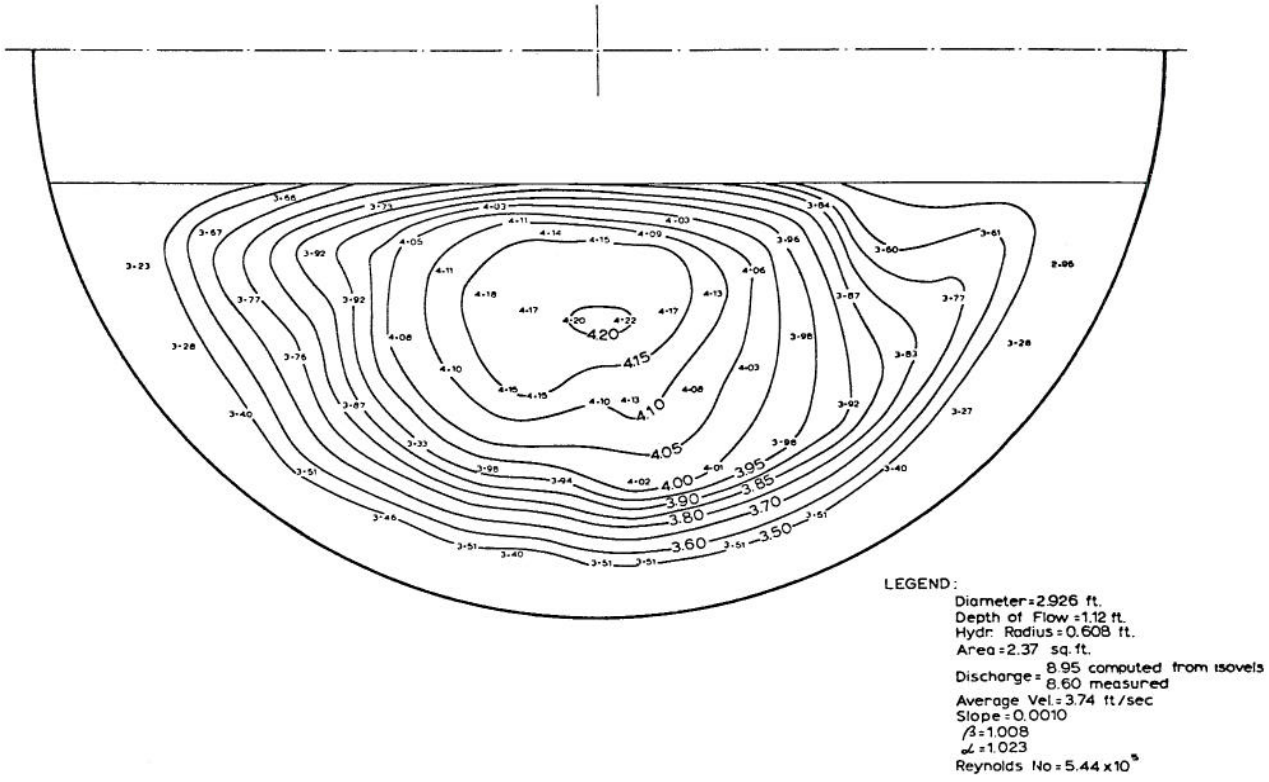

Fig. 5.1. Isovels for partially full pipe flow.

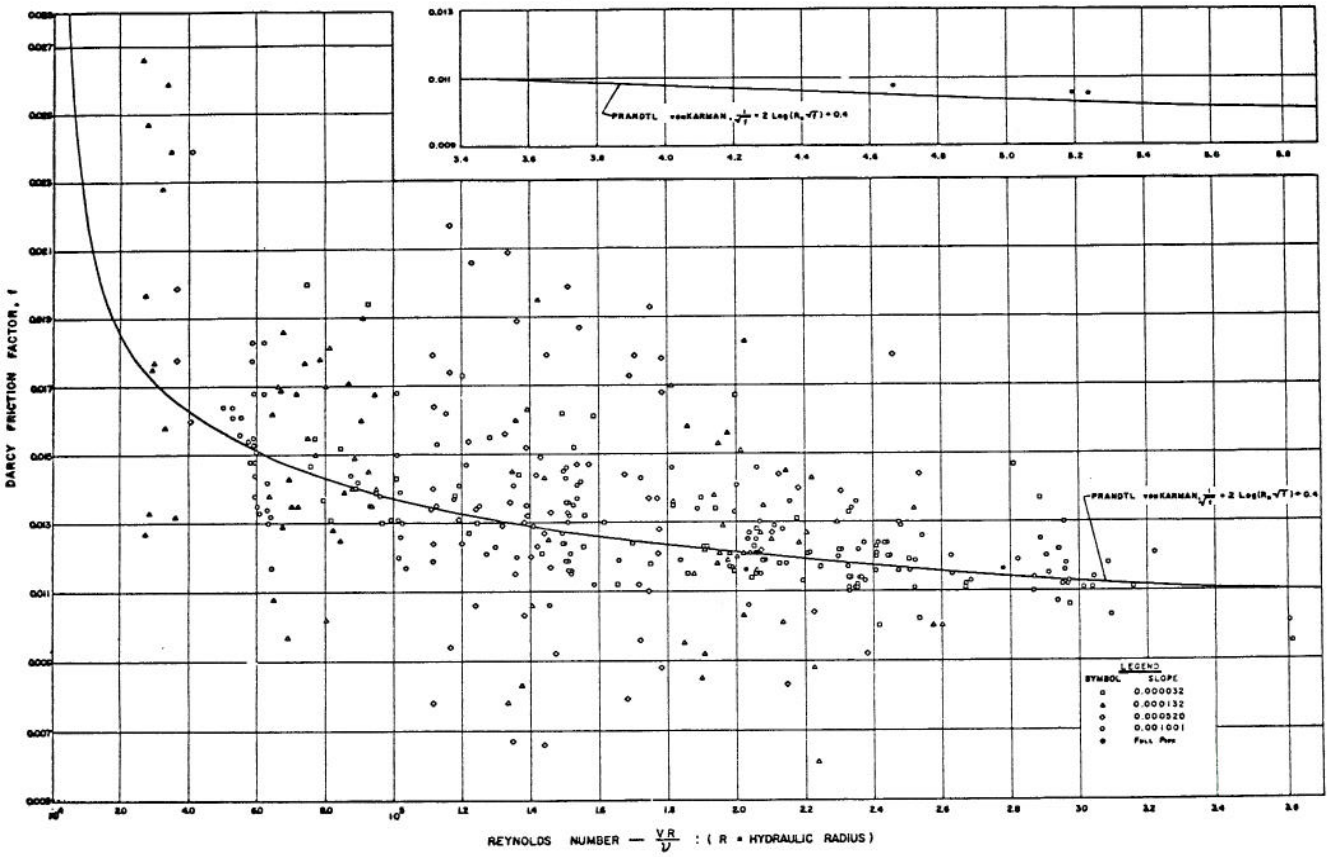

Fig. 5.2. Variation of Darcy-Weisbach friction factor f with the Reynolds number.

For this condition the relation between discharge and depth was determined to be

$$Q = 4.84\ y^{1.35} \quad . \qquad (5.3)$$

This relation applied for depths between approximately one-third and eight-tenths of full diameter.

This gate configuration and flow relation was used for all subsequent observations and evaluations of boundary conditions in which backwater profiles were the initial condition. No attempt was made to modify this steady state relation for unsteady flows.

For a free outfall the location of the computed critical depth occurs some distance upstream from the end of the conduit. The purpose of experimental measurements was to determine the location of the critical depth. This position then served as the location of the downstream boundary. Water-surface profiles were measured for a range of discharges from 2.10 to 16.62 cfs. The channel slope ranged from 0.000032 to 0.001022 foot per foot.

Table 5.2 presents the 14 conditions of discharge and slope, and the corresponding ratio of the end depth to the computed critical depth. Figure 5.3 presents the water-surface profiles for the same conditions as Table 5.2 and also the locations of the computed critical depth.

TABLE 5.2. Free outfall data
Diameter - 2.926 ft.

Run No.	Slope	Discharge	y_e/y_c
D1A	.001022	2.10	0.731
S2-9	.000132	3.26	0.746
S1-5	.000032	4.14	0.758
D2A	.001022	4.58	0.749
S1-6	.000032	7.96	0.776
S3-9	.000520	7.98	0.764
D3A	.001022	8.26	0.751
S1-7	.000032	11.98	0.761
D4A	.001022	12.92	0.740
S3-10	.000520	15.97	0.739
D5A	.001022	16.02	0.752
S1-8	.000032	16.04	0.726
S2-10	.000132	16.64	0.753
S1-9	.000032	19.62	0.761
		Mean -	0.750

Within the range of observed end depths, the mean ratio of end depth to critical depth was 0.750. The ratio tended to be smaller than the mean for the lower depths.

The location of computed critical depth from the channel end varied from less than 3.5 times critical depth to almost 5.5 times critical depth. A location of 4.5 times critical depth was considered as typical and used in subsequent computations.

Flow regimes. The steady non-uniform flow in subcritical and supercritical regimes were established experimentally in the storm conduit. The steady non-uniform flows (backwater curves) at the hydrograph base discharge were used as initial conditions in computing the unsteady flow equations.

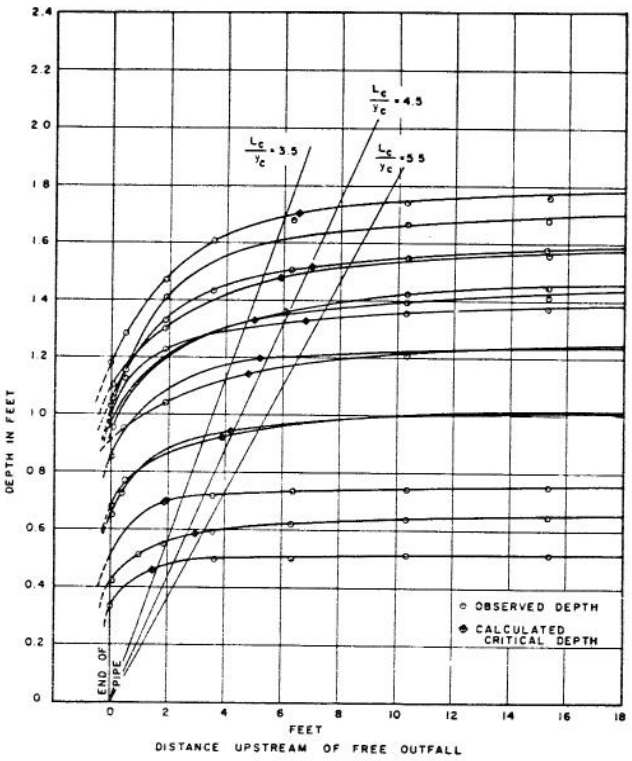

Fig. 5.3. Location of critical depth at the free outfall of a circular cross-section.

The discharge and slope corresponding to the desired depth of flow in subcritical or supercritical regimes were estimated from the previous observations (see Fig. 5.4 and Table 5.3). The downstream control gate was adjusted to produce the desired type of backwater or drawdown curve. Because of the length of time required for steady state conditions to develop, it was not practical to adjust the downstream control until a constant depth developed throughout the length of the pipe. Thus, several conditions of non uniform flow were established both above and below the normal depth. Hook gage readings at the various piezometer locations were made at approximately 15-minute intervals until such time as the readings stabilized.

Water surface elevations were determined by means of hook gage readings taken in gage wells located at 16 positions along the pipe. These wells were connected to the invert of the pipe through a flexible hose. The piezometer openings were 1/16-inch in diameter. At each position there were a sufficient number of openings to insure a reasonable response time for each well.

The invert slope of the pipe was carefully determined by means of a precise self-leveling level with an optical micrometer which permitted measurements of the invert to approximately the nearest 1/1000 of an inch. Readings were taken approximately every 20 feet and a least-square determination of the mean slope was computed. If the maximum deviations at any point exceeded approximately 3/100 of a foot, from the mean line, adjustments to the pipe invert were made.

5.2 Unsteady Flow Conditions

Inflow hydrographs. Inflow hydrographs were developed by manually manipulating a 26-inch diameter ball-valve at the upstream inlet of the main storm

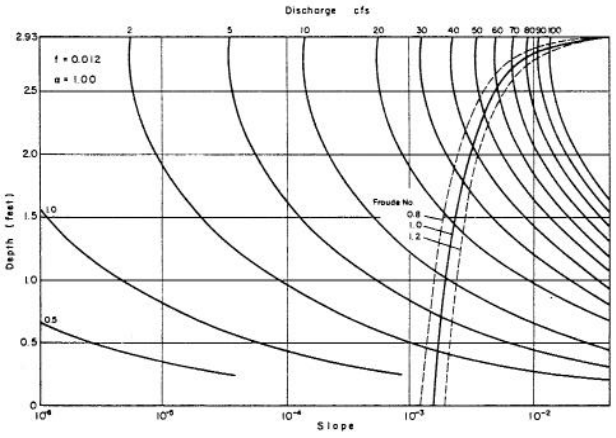

Fig. 5.4. Estimate of discharge versus slope and depth of flow.

conduit and the 12-inch diameter ball-valves on the lateral inflow pipelines. The discharge hydrographs were measured and recorded by pressure transducers connected across the orifices that were installed a short distance downstream of the valves. Figures 5.5 and 5.6 show the experimental observed discharge-inflow hydrographs of the main storm conduit and the lateral flow, respectively.

Wave propagation. After the generation of inflow hydrographs, the subsequent wave depths were measured at several stations downstream as the flood wave propagated along the conduit. Flood wave depths were measured by pressure transducers connected between the conduit invert and a set of manometers.

The measured quantities were plotted as (1) depth versus time relations (Fig. 517), (2) depth versus distance relations (Fig. 5.8), and (3) wave peak depth versus distance and time relations (Fig. 5.9). These relations are later used to check the analytical solutions described in Part I and Part IV of these series of four papers. A summary of the experimental test conditions for the wave measurements are given in Table 5.4.

Effort was made to produce runs which covered a maximum range of base and peak flow discharges. In addition to this, several attempts were made to reproduce the conditions of previous runs so that a measure of expected experimental error might be obtained.

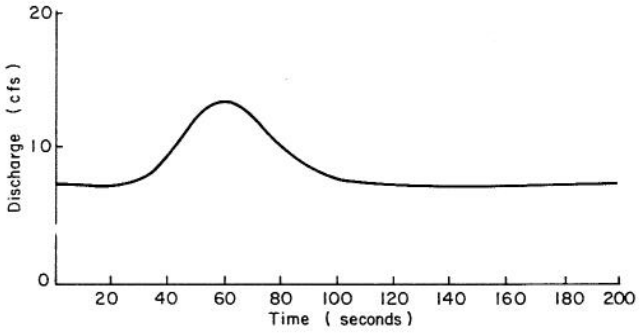

Fig. 5.5. An example of the discharge hydrograph at the upstream inlet of storm conduit.

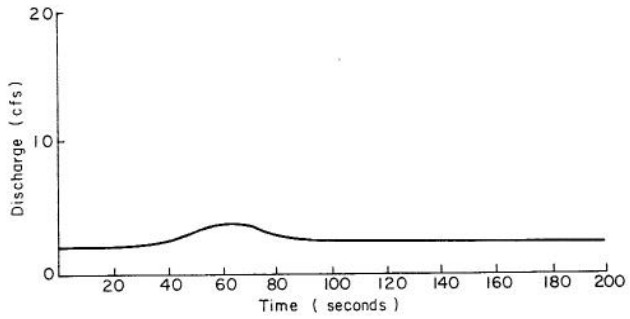

Fig. 5.6. An example of the lateral discharge hydrograph at the junction box being 410.7 feet from the inlet structure to the storm conduit.

TABLE 5.3(a) Operating conditions for June 3-9, 1964[1]

Slope = 0.000132 Run No.	Depth-Diameter Ratio	Normal Depth (ft)	Discharge (cfs)	Gate Condition Open	Gate Condition Closed	Gate Condition Slats	Velocity Traverse Manhole No.	Outlet Profile
B2C	0.3	0.88	3.44			x	2	
B3C	0.4	1.17	4.71			x	2	
B4C	0.5	1.47	5.61			x	2	
B5C	0.6	1.76	10.08			x	2	
B6C	0.7	2.05	15.34			x	2	
B7C	0.8	2.34	18.94			x	2	
B8C	0.9	2.64	19.57			x	2	
B2A	0.3	0.88	3.26	x			2 & 3	x
B6A	0.6	2.05	16.64	x			2, 3 & end	x

[1]In Tables 5.3(a), (b), (c) and (d), each run from which recorded data were obtained has a run number assigned to it. Each run number was indicated in coded form for computer programs as follows:

a. Slope - using letters A, B, C, etc., starting with zero slope as "A".
b. Base discharge - using numbers 1 through 9. 1 corresponding to the lowest and 9 to the highest.
c. Downstream gate position - using letters A, B, C, etc. Letter A represents the free flow (no gate condition); B, gate closed with no slate; and C, D, etc., gate closed with progressively decreasing area by means of the slats.
d. Lateral inflow conditions - using numbers 0 to 9. Zero indicates no lateral inflow, 1-9 will indicate the rate of inflow at each manhole.
e. Unsteady flow conditions - this is either blank, R, or F, depending on whether the flow is of steady, rising, or falling discharge, respectively.
f. Unsteady flow rate-of-change condition - using numbers 1-9 for progressively increasing rates of change of discharge, the longest rate indicated by 1, the highest rate by 9.

TABLE 5.3(b) Operating conditions for June 18-23, 1964

Slope = 0.000520 Run No.	Depth-Diameter Ratio	Normal Depth (ft)	Discharge (cfs)	Gate Conditions Open	Gate Conditions Closed	Gate Conditions Slats	Velocity Traverse Manhole No.	Outlet Profile
C1C	0.2	0.587	1.420			x	2	
C2C	0.3	0.88	2.040			x	2	
C3C	0.4	1.17	6.211			x	2	
C4C	0.5	1.47	7.960			x	2	
C5C	0.6	1.76	10.407			x	2	
C6C	0.7	2.05	14.097			x	2	
C7C	0.8	2.34	12.273			x	2	
C8C	0.9	2.64	18.353			x	2	
C3A	0.4	1.17	7.981	x			2, 3 & end	x
C6A	0.7	2.05	15.972	x			2, 3 & end	x

TABLE 5.3(c) Operating conditions for July 13-17, 1964

Slope = 0.001022 Run No.	Depth-Diameter Ratio	Normal Depth (ft)	Discharge[1] (cfs)	Gate Condition Open	Closed	Slats[2]	Velocity Traverse Manhole No.	Outlet Profile
D1A	.2	.587	2.13	x			2 and end	x
D1B	.2	.587	2.13		x		2	
D1C	.2	.587	2.13			x		
D2A	.3	.88	4.71	x			2 and end	x
D2B	.3	.88	4.71		x		2	
D2C	.3	.88	4.71			x		
D3A	.4	1.17	8.23	x			2 and end	
D3B	.4	1.17	8.23		x		2	
D3C	.4	1.17	8.23			x		
D4A	.5	1.47	12.1	x			2 and end	x
D4B	.5	1.47	12.1		x		2	
D4C	.5	1.47	12.1			x		
D5A	.6	1.76	16.2	x			2 and end	
D5B	.6	1.76	16.2		x		2	
D5C	.6	1.76	16.2			x		
D6A	.7	2.05	20.2	x			2 and end	x
D6B	.7	2.05	20.2		x		2	
D6C	.7	2.05	20.2			x		
D7A	.8	2.34	23.5	x			2 and end	x
D7B	.8	2.34	23.5		x		2	
D7C	.8	2.34	23.5			x		
D8A	.9	2.64	25.7	x			2 and end	x
D8B	.9	2.64	25.7		x		2	
D9A-R1			5-30	Unsteady flow[3] -point gage readings at 1) Upstream end 2) MH 1 3) MH 2 4) MH 3 5) Downstream end				
D9A-F1			30-5					

1 To be set at approximately this value (± 0.2)

2 To produce maximum depth at downstream end.

3 To be repeated enough times to define profile of wave and times of transit.

TABLE 5.3(d) Operating conditions for August 1-8, 1964

Slope = 0.0075 Run No.	Depth-Diameter Ratio	Normal Depth (ft)	Discharge (cfs)	Gate Condition Open	Closed	Slats	Velocity Traverse Manhole No.	Outlet Profile	Remarks
E1A	.2	.587	7.0	x			2 and end	x	
E1B	.2	.587	7.0		x		2		Note location of jump
E2A	.3	.88	16.0	x			2 and end	x	
E2B	.3	.88	16.0		x		2		Note location of jump
E3A	.4	1.17	25.0	x			2 and end	x	
E3B	.4	1.17	25.0		x		2		Note location of jump
E4A	.5	1.47	37.0	x				x	
E4B	.5	1.47	37.0		x		2		"
E5A	.6	1.76	48.0	x			2	x	"
E5B	.6	1.76	48.0		x		2		"
*E6A	.7	2.05	60.0	x				x	"
E6B	.7	2.05	60.0		x		2		"
E7A	.8	2.34	68.0	x			2	x	
E7B	.8	2.34	68.0		x		2		"
E8A	.9	2.64	70.0+	x			2	x	
E8B	.9	2.64	70.0+		x		2		"
E9A			70.0	Unsteady flow-point gage readings at 1) Upstream end 2) MH 1 3) MH 2 4) MH 3 5) Downstream end					

TABLE 5.4. Summary of data on experimental waves at CSU

Run	Slope	Base Flow Depth-Diameter Ratio	Base Flow Discharge (cfs)	Peak Flow Discharge (cfs)	Peak Discharge-Base Flow Ratio	Wave Duration (sec)	Wave Volume (cu-ft)
B2ARS1	.0001100	.21666	1.600	3.870	2.41875	27.000	31.215
B2A0S2	.0001100	.21666	1.540	13.020	8.45455	67.000	382.415
B2A0S3	.0001100	.20846	1.470	15.290	10.40136	78.000	579.665
B3A0S1	.0001100	.37660	4.180	6.940	1.66029	24.000	41.715
B3A0S2	.0001100	.35131	3.490	15.010	4.30086	59.000	473.435
B3A0S3	.0001100	.38993	4.350	17.930	4.12184	83.000	707.330
C2A0S2	.0005500	.16198	2.580	20.330	7.87984	77.000	621.699
C2A0S3	.0005500	.16494	2.410	26.250	10.89212	95.000	986.745
C3A0S1	.0005500	.36849	5.070	14.380	2.83629	42.000	199.295
C3A0S2	.0005500	.36190	4.910	21.920	4.46436	61.000	532.945
C3A0S3	.0005500	.35268	4.990	28.270	5.66533	80.000	924.520
D2ARS1	.0010300	.14729	2.990	19.250	6.43144	60.000	595.650
D2A0S1	.0010300	.15412	2.500	18.550	7.42000	70.000	538.800
D2A0S3	.0010300	.17292	2.990	32.870	10.99331	97.000	1549.860
D3A0S1	.0010300	.37216	7.610	21.450	2.81866	57.000	385.065
D3A0S2	.0010300	.34892	6.940	33.510	4.82853	90.000	1235.095

TABLE 5.4. Summary of data on experimental waves at CSU - (Continued)

Run	Slope	Base Flow Depth-Diameter Ratio	Base Flow Discharge (cfs)	Peak Flow Discharge (cfs)	Peak Discharge-Base Flow Ratio	Wave Duration (sec)	Wave Volume (cu-ft)
D3A0S3	.0010300	.33901	6.330	39.370	6.21959	104.000	1772.335
1 3	.0009900	.34482	6.992	28.071	4.01474	74.740	808.329
1 4	.0009900	.34311	7.592	32.582	4.29163	90.000	1198.544
1 8	.0009900	.20812	1.913	24.396	12.75290	85.470	890.639
1 9	.0009900	.21666	2.602	26.174	10.05925	89.000	1035.399
19909	.0009900	.21290	.904	30.484	35.72119	95.000	1385.264
1 10	.0009900	.20128	2.084	28.326	13.59221	110.000	1348.151
1 11	.0009900	.34994	6.855	22.912	3.34529	60.000	486.608
1 12	.0009900	.34652	6.831	30.655	4.48767	80.000	993.741
1 13	.0009900	.35849	7.280	36.535	5.01300	120.000	1938.801
19913	.0009900	.36464	7.466	36.936	4.94717	110.000	1766.589
0 1	.0009900	.30517	5.439	20.779	3.82037	150.000	1660.597
9 1	.0004800	.24981	2.472	13.577	5.49215	57.000	345.406
9 2	.0004800	.25152	2.336	20.338	0.01970	94.000	995.381
9 3	.0004800	.33336	5.033	15.214	3.02284	53.000	277.884
9 4	.0004800	.35885	5.292	22.349	4.22307	107.000	1090.523

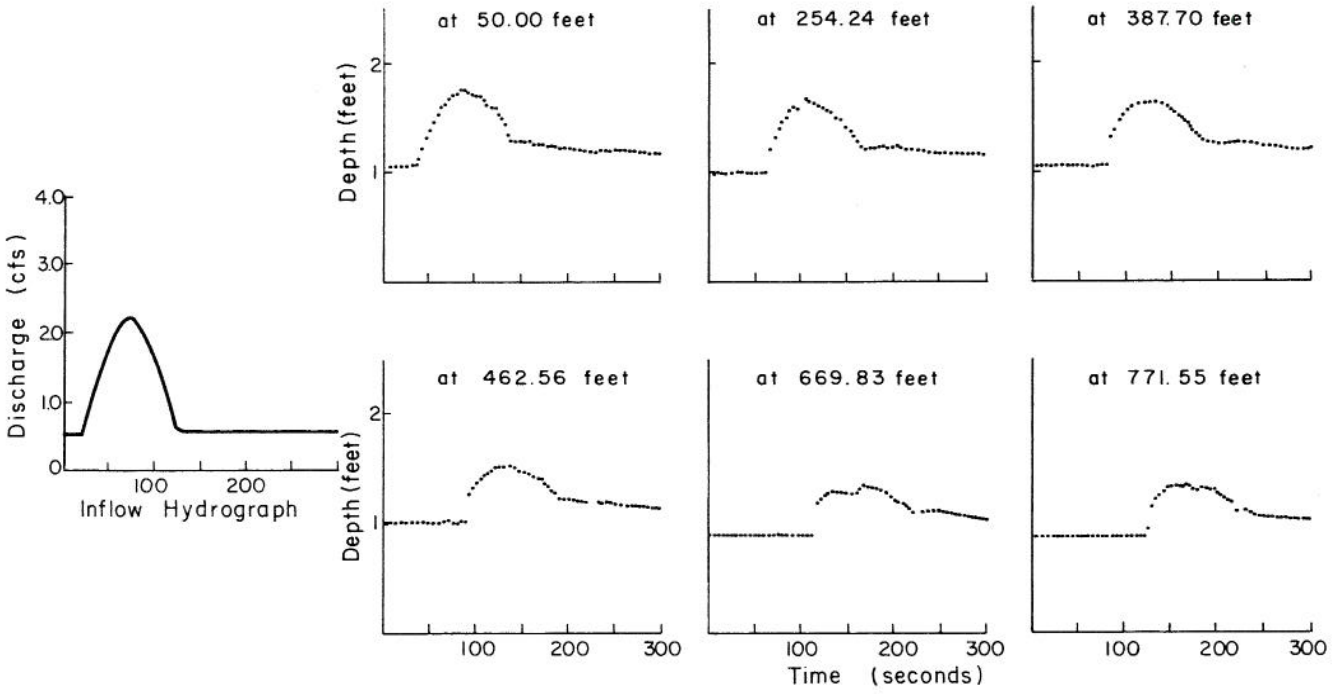

Fig. 5.7. Observed wave forms given as depth versus time, computer plotted, Run No. 090004, S_o = 0.00048.

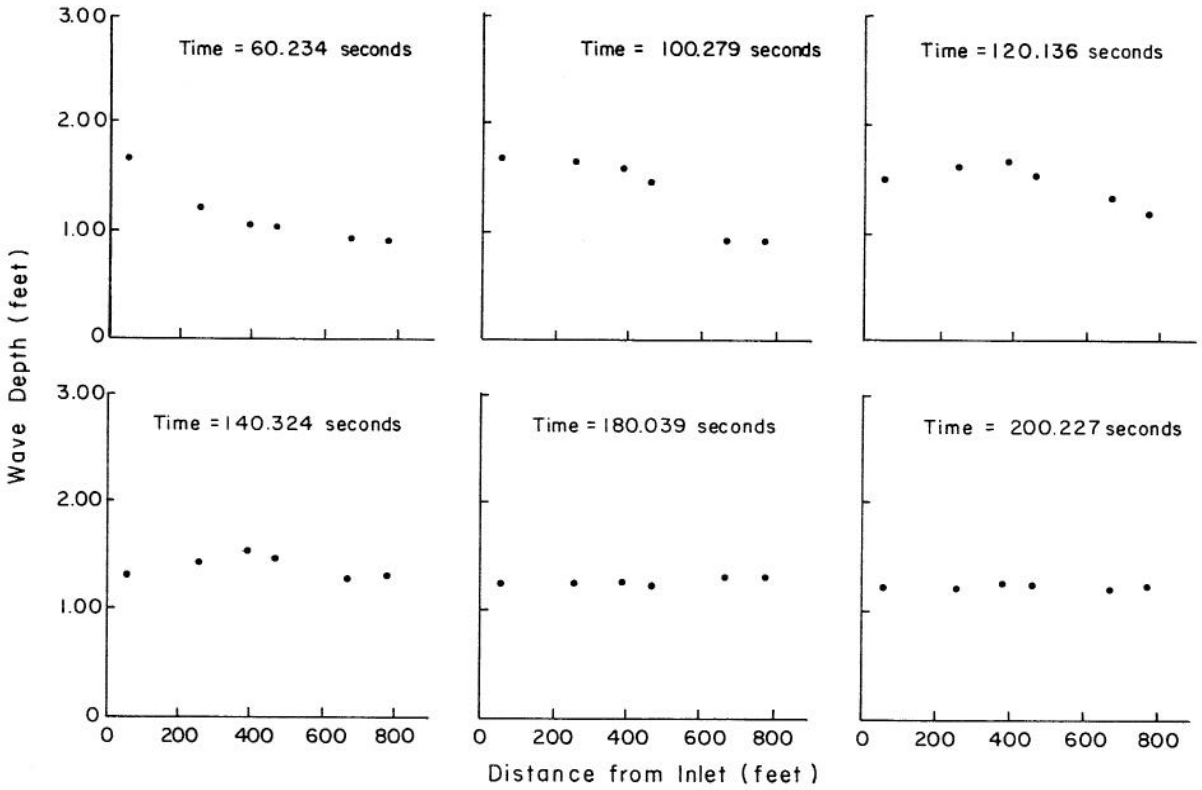

Fig. 5.8. Observed wave forms given as depth versus distance, computer plotted, Run No. 090004, S_o = 0.00048.

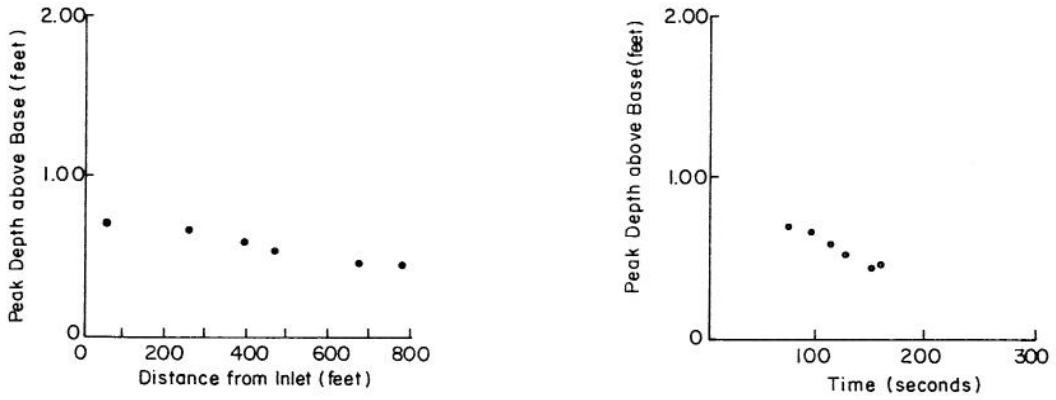

Fig. 5.9. Observed hydrograph peak depths versus the distance (left graph) or versus the time (right graph), computer plotted, Run No. 090004, S_o = 0.00048.

Chapter 6

EXPERIMENTAL ERRORS

6.1 Errors in Geometric Variables

The steel conduit used as an open channel for the data analyzed herein was 3-feet in diameter, 1/2-inch thick rolled-plate with a longitudinal welded joint. The 20-foot sections were butt-welded together and were supported on steel rails at approximately 20-foot spacing, not necessarily at the conduit joints. As a result of the manufacturing process, handling, field welding, and the method of support it was not expected that the conduit would be perfectly circular or possess a straight line invert profile. The errors caused by physical departures from the mathematical geometric forms in the conduit cross-section and longitudinal invert slope are discussed here.

Conduit cross-sectional irregularities. Measurements were made on the inside diameter of the pipe at 60 degree intervals to the nearest 0.001 inch, both before and after painting the inside of the pipe. Before the inside of the pipe was painted measurements were made at cross sections spaced 20-feet apart. After painting, similar measurements were made at 10-ft. intervals. An elliptical cross-section (Fig. 6.1) was assumed and the corresponding major axis (a), minor axis (b), the direction of the principal axes (α), eccentricity ($e = \sqrt{1 - (a/b)^2}$), area, wetted perimeter, and hydraulic radius were computed based on the three measured diameters at each cross-section and its orientation angle (Table 6.1). The differences between the means of each of the parameters for the two surveys are not significant on the 5 percent level. This would indicate (1) that painting the pipe had no effect on the internal geometry, and (2) that doubling the number of stations did not significantly improve knowledge about the geometry of the pipe.

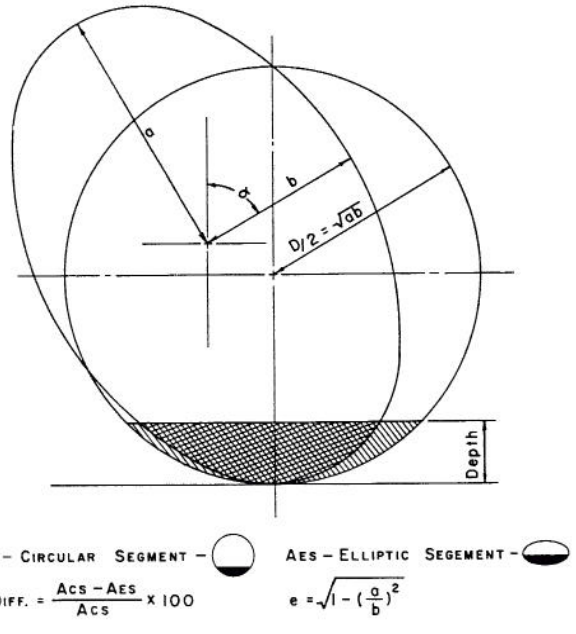

Fig. 6.1. Definition sketch for the relation of the circular and the elliptical cross-sections.

TABLE 6.1. Conduit geometry

	No. of Stations	Maximum	Mean	Minimum	Standard Deviation
Major Axis-(inches)	40	17.869	17.617	17.538	0.175
	84	17.913*	17.604	17.554	0.047
Minor Axis-(inches)	40	17.626	17.516	17.435	0.0375
	84	17.680	17.510	17.430	0.031
Eccentricity	40	0.176	0.1021	0.046	0.0310
	84	0.175	0.0993	0.051	0.0244
Alpha-(degrees)	40	165.58	84.84	13.71	46.5
	84	160.37	82.95	7.78	49.43
Area-(inch^2)	40	989.5	969.47	965.3	3.84
	84	994.9*	968.4	964.1*	3.94
Wetted Perimeter (inches)	40	111.51	110.373	110.13	0.2769
	84	111.82*	110.314	110.07*	0.2167
Hydraulic Radius (inches)	40	8.87	8.7785	8.76	0.0183
	84	8.89*	8.7742	8.75*	0.0181

* Occurred at same section

Accepting an average area of 968.41 square inches (6.725 sq ft) the mean diameter for the pipe is then 2.9262 feet. This figure was used for the pipe diameter in all subsequent calculations.

The eccentricity and the angle alpha for the observed geometry of the pipe serve as a means to estimate the possible error in subsequent hydraulic calculations. The percent difference between the circular and elliptical segments for the maximum and mean eccentricity at a depth ratio of 0.2 was determined and plotted in Fig. 6.2 as a function of the angle α. As may be seen from this plot, the error in area becomes a maximum at angular positions of zero and 90 degrees. For the mean eccentricity for a pipe of this depth ratio, the maximum error is 1.1 percent. For the mean α-angle of about 85 percent, the maximum error for the mean eccentricity is approximately 1 percent.

In view of the interrelated effects of depth, eccentricity, and α, it appears that an error in the computation of the flow area caused by assuming a circular cross section instead of an approximated ellipse, may range from 0 to 3 percent with 1 percent being representative.

Conduit invert slope irregularities. Another source of geometric error are inherent irregularities in the experimental conduit slopes. Conservation of energy dictates that for subcritical flow, depth must increase over channel depressions and decrease over channel rises. This fluctuation in depth resulted in observed depth values that differed from the corresponding theoretical depth values that had been computed assuming a perfectly constant invert slope. For computational purposes, the average values of experimental slopes were determined by running precision

level surveys along the pipe's invert and applying a least-square analysis to the elevation points obtained. This was accomplished by first adjusting the pipe to a predetermined position on the supporting rails and then leveling the pipe with a self-leveling level having an optical micrometer of at least count of 0.001 inch. The invert elevations were observed at 45 positions approximately 20 feet apart. A least-square determination of the slope and the deviations at each position was then made. If the deviations displayed a consistent or excessive trend in a given length, that portion of the conduit was readjusted, and the elevations redetermined.

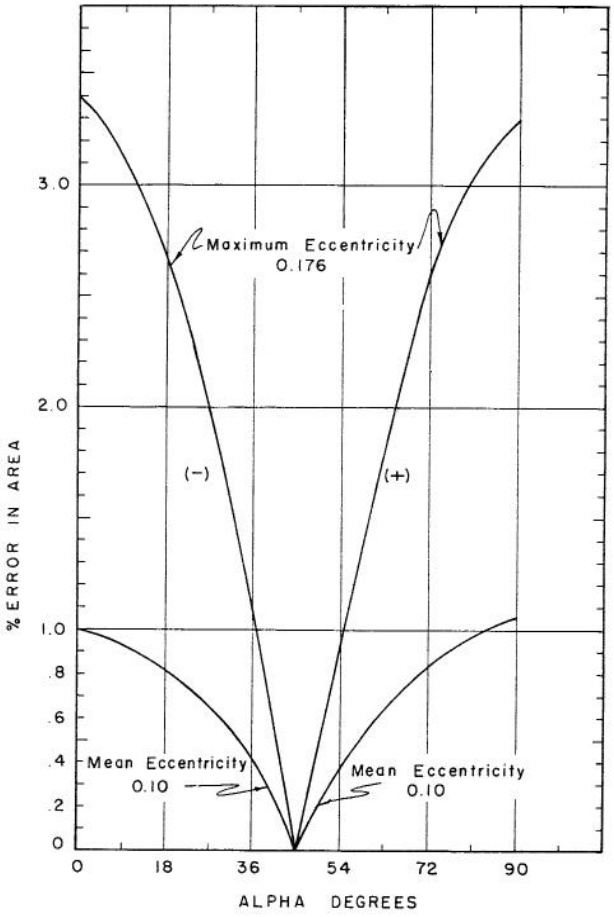

Fig. 6.2. Percent error in area of the storm conduit. (at the depth ratio of 0.2).

The standard deviations of the actual invert profile points about these least-square slopes are given in Table 6.2, and profiles of the conduit's invert for representative slopes are shown in Figs. 6.3 and 6.4. It may be concluded that for the slopes investigated, the observed depths may deviate from the ideal depths by an average of 0.01 to 0.03 ft.

6.2 Time-Difference Errors

A systematic error was introduced into all tests because the flow-measuring orifice was located 82.2 feet upstream of what was considered the beginning of the test conduit. For much of this distance the conduit was flowing full and providing instantaneous transmission of changes in flow. The distance between the point where a free surface formed and the beginning point of the test conduit, however, provided a varying time lag between observed and computed data of from 8 to 14 seconds. That is, the time recorded by the orifice transducer for a given flow discharge led the time when that discharge actually reached the conduit test section by the amount of time it took for the wave to travel the 82.2 feet. To eliminate this difference in the comparisons, time lags were estimated visually from comparison of observed and computed waves (depth versus time) and all experimental times were adjusted by this amount.

TABLE 6.2. Data for Colorado State University experimental conduit invert slopes

Slope	Standard Deviation - Ft
0.0001110	0.0141
0.0005487	0.0141
0.001033	0.0136
0.0009930	0.0180
0.0004848	0.0213
0.0000052	0.0116
0.0000157	0.0135
0.0000303	0.0099
0.0001325	0.0099
0.0005197	0.0117
0.0010101	0.0119
0.0074578	0.0133
0.0200690	0.0141

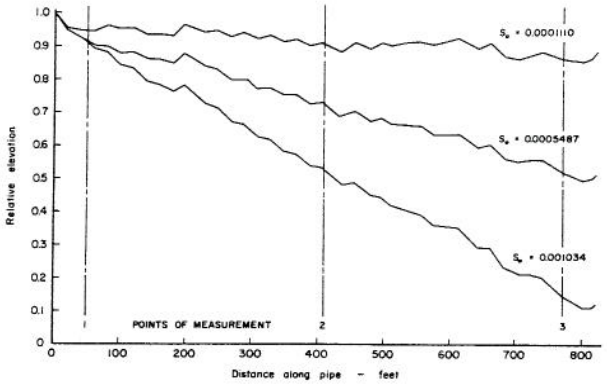

Fig. 6.3. Invert profiles for Colorado State University experimental storm conduit (1965).

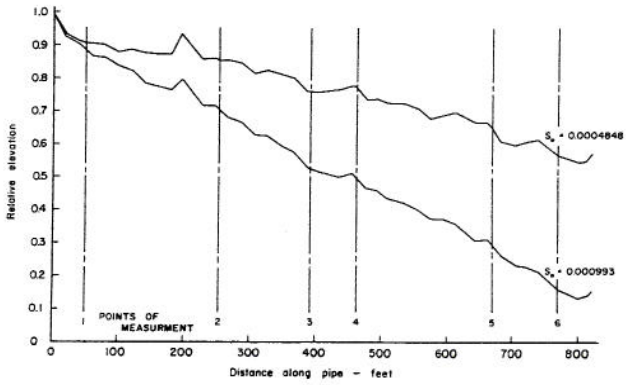

Fig. 6.4. Invert profiles for Colorado State University experimental storm conduit (1966).

6.3 Instrumentation Errors

Instrumentation errors were analyzed on the basis of calibration results. Since the true values of physical quantities can never be exactly measured, the calibration process of each instrument was considered to be an accurate estimate of the errors in the measured quantities.

A common method of giving bounds on the errors uses the standard deviation s defined by

$$s^2 = \sum_{i=1}^{N} \frac{(q_i - q_o)^2}{N - 1} \quad , \qquad (6.1)$$

in which q_i is the individual reading observed in a given range, q_o is the corresponding reading from a reference curve in the same given range as q_i and N is the total number of observations.

For a Gaussian distribution of errors and a significance level, the physical quantities measured by each instrument can then be expressed as

$$q_o = q_i \pm 2\,s \quad . \qquad (6.2)$$

Equation 6.2 means that approximately 95 percent of the measured quantities q_i lie within the range of $\pm$ 2 s of q_o.

Table 6.3 gives a summary of the calibration results of the orifice meters, current meters, and pressure transducers (as described in Chapter 3) by using Equation 6.2.

6.4 Reproducibility Errors

As stated earlier, an attempt was made to perform some experiments having conditions exactly the same as conditions of some selected previous runs. This was done to have some measure of the errors due to reproducibility inherent in the experimental system. By running two runs under exactly the same conditions, the differences between the observed wave forms and the observed wave depths would be a measure of this type of error. If no errors were generated by the system, the observed values for both runs would be the same. This manner of comparison would not, however, measure the random errors.

During the experiments, seven attempts were made to duplicate the conditions of previous runs. Only one of these runs, however, actually duplicated previous conditions. The other six runs could not be used in this evaluation because either the base or peak flows did not correspond to the earlier conditions or the time of one wave was longer than that of the previous run resulting in different total water volumes. The runs with matching conditions were 010013 and 019913.

To measure the differences between the two sets of observed data on the flood hydrographs, relative errors between the two areas of each of the six different observed wave forms (depth versus time) were computed. Corresponding relative errors between the two computed areas were obtained. The resulting average error of reproducibility was 5.86 percent.

Another measure of errors of reproducibility was obtained by computing the relative errors between corresponding maximum depth values at each of the six observation positions. For exactly the same inflow hydrographs, these errors should be zero. The average of the errors, however, is 8.13 percent. Again, the effect of the difference in inflow hydrographs was removed. In this case, the average relative error between the two computed conditions was 1.47 percent. The average error of reproducibility computed this way was 6.66 percent.

Observed values for the depth versus distance relations were not compared because of the influence on these depths by the experimental time shifts. An error of one or two seconds in the determination of these shifts could introduce errors as high as $\pm$0.1 foot to the observed depths. Other relations for the depth versus time data were not compared because of their dependence on the exact positioning of the observed peaks. The two errors may be combined to give an average error of reproducibility of approximately 6 percent.

TABLE 6.3. Estimate of instrumentation errors

		Figure or Table in Chapter 3	s Standard Deviation	Error Bounds with 2.5% Level	Range
Orifice Meters	Small Opening	Fig. 3.1	0.00413	$\alpha = \alpha \pm 0.00826$	Reynolds no. $3\times10^5 \sim 2\times10^6$
	Medium Opening	Fig. 3.1	0.00220	$\alpha = \alpha \pm 0.00440$	Reynolds no. $2\times10^5 \sim 2\times10^6$
	Large Opening	Fig. 3.1	0.00320	$\alpha = \alpha \pm 0.00640$	Reynolds no. $5\times10^5 \sim 2\times10^6$
	Large Opening	Fig. 3.2	0.01619 ft^3	$\forall = \forall \pm 0.03238\ ft^3$	Volume 8 $\sim$ 15 ft^3
Current Meters		Table 3.1	0.0141 ft/sec	$V = V \pm 0.0282$ ft/sec	Velocity 1 $\sim$ 8 ft/sec
		Table 3.1	0.0451 ft/sec	$V = V \pm 0.0902$ ft/sec	Velocity 8 $\sim$ 16 ft/sec
Pressure Transducers		Fig. 3.12	0.0002 ft of water	$H = H \pm 0.0004$ ft of water	Pressure $\pm$ 1 psi Voltage $\pm$ 3 volts
		Fig. 3.13	0.0003 ft of water	$H = H \pm 0.0006$ ft of water	Pressure $\pm$ 5 psi Voltage $\pm$ 3 volts

Chapter 7

EVALUATION OF EXPERIMENTAL FACILITIES

7.1 Summary of Characteristics of Experimental Facilities

(1) The large scale conduit experimental research facilities made it possible to carry out experiments with discharges ranging up to approximately 70 cubic feet per second and with depths of free-surface flow up to the full pipe diameter of 3 feet.

(2) The slope of the conduit can be varied from zero to 5 percent which covers the subcritical flow range as well as part of the supercritical range.

(3) Instrumentation was selected for maximum accuracy and reliability under field conditions.

(4) Calibration of instruments was carried to the point of reducing errors to practical, feasible minimums.

(5) A data acquisition analog-to-digital system was designed and constructed with outputs in a form ready for computation in digital computers.

(6) The facilities were designed such that all basic geometric and hydraulic properties can be measured with maximum accuracy.

(7) The facilities were designed so that accurate observations of a generated flood hydrograph at the inlet and the depth hydrographs at selected positions along the conduit, rather than for a precise reproduction of flood waves could be made.

(8) Typical experimental data are considered sufficiently accurate for analysis and synthesis of both the geometric and hydraulic conditions of the conduit and waves, as well as for comparison of numerically integrated and measured waves.

(9) Although the experimental facilities were built in the Outdoor Laboratory as described in Chapter 2, tests were conducted only during the summer months with air temperature in the range of 65^{o}-85^{o}F. No significant effects due to the differences in climatic conditions were observed.

7.2 Potential of Facilities for Further Experimental Investigations

Experience with the designed and constructed experimental research facilities indicates that the following subjects may be studied effectively, and eventually warrant further investigation or verification on these facilities:

(1) Friction losses in unsteady free-surface flow as compared to losses in steady uniform flow could be studied, after the further theoretical investigations have been undertaken, and the new experimental methods conceived and designed beyond all previous works.

(2) Experiments studying the movement of hydraulic bores through storm drains when the long flood waves pass to bores may have practical significance. If so, this significance can be checked through new analytical derivations made by experimental observations; for example, how the shape and friction factors of storm drains affect this movement.

(3) Experiments for better understanding the modification of flood waves in a complex conduit, such as changes in conduit cross-sections, bottom irregularities, presence of local humps or similar obstructions could be conducted.

(4) Experiments with the propagation of flood waves in a dry storm drain will contribute to a better understanding of this phenomenon.

(5) Experiments could be conducted to better understand and describe particular end boundary conditions, which can occur in practice with storm drains.

(6) Experiments of flow close to full cross-sections would permit an evaluation of conditions for full flow or intermittent full flow, free surface flow.

(7) Specially designed experiments of partially full steady flow would permit an evaluation of the air transported by the surface drag and the accompanying pressure reduction within the free space of the pipe.

REFERENCES

External References

1. Henn, W., Fundamentals of Hydrometry with Propeller Current Meters (in German). Forschungsh. Ver. dtsch. Ing., 1937, 8(385), 1-22.

2. Staus, A., Die Genauigkeit von Flugelmessungen bei Wasser Kraftanlagen. (The accuracy of current meter measurements at hydraulic power stations.) Berlin: Springer, 1926.

3. Jovanovic, S., Current Meter. Theory, rating and precision of measuring. Monographs, 6. Belgrade: Institute of Hydraulic Engineering.

4. Benini, G., Experimental Research on Current Meters Carried out in the Rating Tank (in Italian). 5th Congress on Hydraulics. Turin, 1957.

Internal References

From the Project Reports and Theses

1. Yevjevich, V. M., June 1961, "Unsteady Free Surface Flow in a Storm Drain" - General and Analytical Study. Report for the U. S. Bureau of Public Roads, Eng. Research Center, Colorado State University. CER61-VMY38.

2. Barnes, A. H., August 1965, "Predictability of Free-Surface Profiles for Steady Non-uniform Flow in a Circular Cross-Section", Ph.D. dissertation, Dept. of Civil Eng., Colorado State University.

3. Lorah, W. L., June 1966, "Free-Surface Flow Energy Losses in a 90^{o} Junction Box", M.S. Thesis, Dept. of Civil Eng. Colorado State University.

4. Yevjevich, V. M. & Barnes, A. H., August 1966, "Hydraulic Roughness of Free-Surface Flow in a Smooth Steel Pipe", Report for U.S. Bureau of Public Roads, Eng. Research Center, Colorado State University.

5. Barnes, A. H., October 1966, "Velocity Distribution Factors in a Circular Cross-Section", Report for U.S. Bureau of Public Roads, Eng. Research Center, Colorado State University.

6. Pinkayan, S. & Barnes, A. H., Feb. 1967, "Unsteady Free-Surface Flow in a Storm Drain with Lateral Inflows", Report for U. S. Bureau of Public Roads, Eng. Research Center, Colorado State University.

7. Mitchell, J. S., April 1967, "Comparison of Mathematical versus Experimental Flood Wave Attenuation in Part-full Pipes", M.S. Thesis, Dept. of Civil Eng., Colorado State University. Also prepared as a report for U.S. Bureau of Public Roads.

8. Barnes, A. H., June 1969, "Unsteady Flow in a Storm Drainage System, Part A - Theory and Error Considerations", Report for U.S. Bureau of Public Roads, Eng. Research Center, Colorado State University. CER69-70AB1.

9. Barnes, A. H., January 1970, "Unsteady Flow in a Storm Drainage System, Part B - Hydraulic Parameters, Boundary and Initial Conditions", Report for U.S. Bureau of Public Roads, Eng. Research Center, Colorado State University. CER69-70AB1.

Key Words: Storm Drain, Flood Routing, Unsteady Flow, Wave Propagation.

Abstract: This second part of a four-part series of hydrology papers on flood routing through storm drains relates exclusively to experimental research facilities and experiments. The following subjects are presented: (a) design and construction of the experimental storm drain system as a special research outdoor facility: (b) instrumentation and its calibration: (c) description of the data recording system; (d) various experimental test conditions and their typical results, and (e) discussion of experimental errors.

A large conduit, 3 feet in diameter and 822 feet long, has been selected, designed, and constructed in the Outdoor Laboratory of Colorado State University to accurately measure geometric and hydraulic characteristics, as well as the propagating of flood waves. Instrumentation has been selected to suit the field conditions. The calibration of the instruments has been carried out to the point where there are relatively small errors. The data recording system was designed and constructed so that the output could be put either on cards or paper tapes and provide a direct input for computations on a digital computer. Only typical results of experiments carried out are described in this paper; experimental errors are reviewed in a summarized form.

Reference: Yevjevich, Vujica and Albert H. Barnes, Colorado State University, Hydrology Paper No. 44 (November 1970) "Flood Routing Through Storm Drains, Part II, Physical Facilities and Experiments.

Key Words: Storm Drain, Flood Routing, Unsteady Flow, Wave Propagation.

Abstract: This second part of a four-part series of hydrology papers on flood routing through storm drains relates exclusively to experimental research facilities and experiments. The following subjects are presented: (a) design and construction of the experimental storm drain system as a special research outdoor facility: (b) instrumentation and its calibration: (c) description of the data recording system; (d) various experimental test conditions and their typical results, and (e) discussion of experimental errors.

A large conduit, 3 feet in diameter and 822 feet long, has been selected, designed, and constructed in the Outdoor Laboratory of Colorado State University to accurately measure geometric and hydraulic characteristics, as well as the propagating of flood waves. Instrumentation has been selected to suit the field conditions. The calibration of the instruments has been carried out to the point where there are relatively small errors. The data recording system was designed and constructed so that the output could be put either on cards or paper tapes and provide a direct input for computations on a digital computer. Only typical results of experiments carried out are described in this paper; experimental errors are reviewed in a summarized form.

Reference: Yevjevich, Vujica and Albert H. Barnes, Colorado State University, Hydrology Paper No. 44 (November 1970) "Flood Routing Through Storm Drains, Part II, Physical Facilities and Experiments.

Key Words: Storm Drain, Flood Routing, Unsteady Flow, Wave Propagation.

Abstract: This second part of a four-part series of hydrology papers on flood routing through storm drains relates exclusively to experimental research facilities and experiments. The following subjects are presented: (a) design and construction of the experimental storm drain system as a special research outdoor facility: (b) instrumentation and its calibration: (c) description of the data recording system; (d) various experimental test conditions and their typical results, and (e) discussion of experimental errors.

A large conduit, 3 feet in diameter and 822 feet long, has been selected, designed, and constructed in the Outdoor Laboratory of Colorado State University to accurately measure geometric and hydraulic characteristics, as well as the propagating of flood waves. Instrumentation has been selected to suit the field conditions. The calibration of the instruments has been carried out to the point where there are relatively small errors. The data recording system was designed and constructed so that the output could be put either on cards or paper tapes and provide a direct input for computations on a digital computer. Only typical results of experiments carried out are described in this paper; experimental errors are reviewed in a summarized form.

Reference: Yevjevich, Vujica and Albert H. Barnes, Colorado State University, Hydrology Paper No. 44 (November 1970) "Flood Routing Through Storm Drains, Part II, Physical Facilities and Experiments.

Key Words: Storm Drain, Flood Routing, Unsteady Flow, Wave Propagation.

Abstract: This second part of a four-part series of hydrology papers on flood routing through storm drains relates exclusively to experimental research facilities and experiments. The following subjects are presented: (a) design and construction of the experimental storm drain system as a special research outdoor facility: (b) instrumentation and its calibration: (c) description of the data recording system; (d) various experimental test conditions and their typical results, and (e) discussion of experimental errors.

A large conduit, 3 feet in diameter and 822 feet long, has been selected, designed, and constructed in the Outdoor Laboratory of Colorado State University to accurately measure geometric and hydraulic characteristics, as well as the propagating of flood waves. Instrumentation has been selected to suit the field conditions. The calibration of the instruments has been carried out to the point where there are relatively small errors. The data recording system was designed and constructed so that the output could be put either on cards or paper tapes and provide a direct input for computations on a digital computer. Only typical results of experiments carried out are described in this paper; experimental errors are reviewed in a summarized form.

Reference: Yevjevich, Vujica and Albert H. Barnes, Colorado State University, Hydrology Paper No. 44 (November 1970) "Flood Routing Through Storm Drains, Part II, Physical Facilities and Experiments.

PREVIOUSLY PUBLISHED PAPERS OF VOLUME 2

Colorado State University Hydrology Papers

No. 26 "The Investigation of Relationship Between Hydrologic Time Series and Sun Spot Numbers," by Ignacio Rodriguez-Iturbe and Vujica Yevjevich, April 1968.

No. 27 "Diffusion of Entrapped Gas From Porous Media," by Kenneth M. Adam and Arthur T. Corey, April 1968.

No. 28 "Sampling Bacteria in a Mountain Stream," by Samuel H. Kunkle and James R. Meimann, March 1968.

No. 29 "Estimating Design Floods from Extreme Rainfall," by Frederick C. Bell, July 1968.

No. 30 "Conservation of Ground Water by Gravel Mulches," by A.T. Corey and W.D. Kemper, May 1968.

No. 31 "Effects of Truncation on Dependence in Hydrologic Time Series," by Rezaul Karim Bhuiya and Vujica Yevjevich, November 1968.

No. 32 "Properties of Non-Homogeneous Hydrologic Series," by V. Yevjevich and R.I. Jeng, April 1969.

No. 33 "Runs of Precipitation Series," by Jose Llamas and M.M. Siddiqui, May 1969.

No. 34 "Statistical Discrimination of Change in Daily Runoff," by Andre J. Dumas and Hubert J. Morel-Seytoux, August 1969.

No. 35 "Stochastic Process of Precipitation," by P. Todorovic and V. Yevjevich, September 1969.

No. 36 "Suitability of the Upper Colorado River Basin for Precipitation Management," by Hiroshi Nakamichi and Hubert J. Morel-Seytoux, October 1969.

No. 37 "Regional Discrimination of Change in Runoff," by Viboon Nimmannit and Hubert J. Morel-Seytoux, November 1969.

No. 38 "Evaluation of the Effect of Impoundment on Water Quality in Cheney Reservoir," by J.C. Ward and S. Karaki, March 1970.

No. 39 "The Kinematic Cascade as a Hydrologic Model," by David F. Kibler and David A. Woolhiser, February 1970.

No. 40 "Application of Run-Lengths to Hydrologic Series," by Jaime Saldarriaga and Vujica Yevjevich, April 1970.

No. 41 "Numerical Simulation of Dispersion in Groundwater Aquifers," by Donald Lee Reddell and Daniel K. Sunada

No. 42 Theoretical Probability Distributions for Flood Peaks, Emir Zelenhasic, December 1970.

No. 43 "Flood Routing Through Storm Drains, Part I, Solution of Problems of Unsteady Free Surface Flow in a Storm Drain", by V. Yevjevich and A.H. Barnes.